**Quarterly Progress Report**

**High Temperature Electrochemical Polishing of $H_2S$**

**from Coal Gasification Process Streams**

**Grant DE-FG22-94-PC94207**

**July 1, 1997 - September 30, 1997**

**by**

**Professor Jack Winnick**

**Georgia Institute of Technology**

**School of Chemical Engineering**

**Atlanta, GA  30332-0100**

## Disclaimer

## Abstract

An advanced process for the separation of hydrogen sulfide from coal gasification streams through an electrochemical membrane is being perfected. $H_2S$ is removed from a synthetic gas stream, split into hydrogen, which enriches the exiting syn-gas, and sulfur, which is condensed downstream from an inert sweep gas stream. The process allows for continuous removal of $H_2S$ without cooling the gas stream while allowing negligible pressure loss through the separator. Moreover, the process is economically attractive due to the elimination of the need for a Claus process for sulfur recovery. To this extent the project presents a novel concept for improving utilization of coal for more efficient power generation.

# Table of Contents

## Executive Summary

This quarter focused on two specific materials issues involved with the Electrochemical Membrane Separator (EMS): passivation of stainless steel cell housings, and alternative cathode materials. Stainless steel cell housings which had been aluminum plasma coated were again tested in full cell runs, in order to determine the effectiveness of carbonate transport and $H_2S$ removal. It was anticipated that the aluminum layer would oxidize to alumina and provide a passivation layer which passivated the cell housings to eliminate the possibility of parasitic reactions at the current carrying cell housings. The EMS was successful at carbonate transport in all cell runs utilizing the stainless steel cell housings, and $H_2S$ removal was observed in one of these runs. All runs were plagued by electrolyte mismanagement which led to flooded cathodes. Hence, current efficiencies were diminished at higher applied currents.

Other research this quarter involved preliminary work in determining alternative cathode materials for nickel. Previously, full cell EMS runs were carried out at 580 °C in order to avoid the nickel sulfide liquid eutectic which occurs when the nickel cathode is subject to $H_2S$ above 600 °C. This quarter, $LiCoO_2$ was studied as an alternative cathode material which will be stable at 650 °C. $LiCoO_2$ was synthesized in this lab via the solid state reaction. Electrodes were fabricated by dry pressing and then sintering. One full cell run was attained in which the $LiCoO_2$ cathode achieved stoichiometric $CO_2$ removal. $H_2S$ removal was also observed with this cathode.

## Project Objectives

Coal may be used to generate electrical energy by any of several processes, most of which involve combustion or gasification. Combustion in a coal-fired boiler and power generation using a steam-cycle is the conventional conversion method; however total energy conversion efficiencies for this type of process are only slightly over 30%[1]. Integration of a gas-cycle in the process (combined cycle) may increase the total conversion efficiency to 40%[1]. Conversion processes based on gasification offer efficiencies above 50%[1].

$H_2S$ is the predominant gaseous contaminant in raw coal gas. Coal depending on the type and area of extraction can contain up to 5 wt% sulfur, which is converted to gaseous $H_2S$ during gasification. Problems arise due to the corrosive nature of $H_2S$ on metal components contained in these cycles. Because of this, $H_2S$ concentrations must be reduced to low levels corresponding to certain power applications. For example, an integrated coal gasification-combined cycle (IGCC) process producing electricity from coal at nearly 50% overall efficiency[1] incorporates gas turbines that cannot tolerate $H_2S$ levels above 100 ppm. Coal gasification/Molten Carbonate Fuel-Cell(MCFC) systems, achieving conversion efficiencies around 60%[2], function properly only if $H_2S$ is below 1 ppm.

An advanced process for the separation of hydrogen sulfide ($H_2S$) from coal gasification product streams through an electrochemical membrane is being developed using funds from this grant. $H_2S$ is removed from the syn-gas stream, split into hydrogen, which enriches the exiting syn-gas, and sulfur, which is condensed from an inert sweep gas stream, Figure 1. The process allows removal of $H_2S$ without cooling the gas stream and with negligible pressure loss through

the separator. The process is made economically attractive by the lack of need for a Claus process for sulfur recovery. To this extent the project presents a novel concept for improving utilization of coal for more efficient power generation.

Past experiments using this concept dealt with identifying removal of 1-2% $H_2S$ from gases containing only $H_2S$ in $N_2$[3], simulated natural gas[4,5], and simulated coal gas[6]. Data obtained from these experiments resulted in extended studies into electrode kinetics and electrode stability in molten melts[7,8,9]. The most recent experiments evaluated the polishing application (removal of $H_2S$ below 10 ppm) using the Electrochemical Membrane Separator (EMS). $H_2S$ removal efficiencies over 90% were achieved at these stringent conditions of low $H_2S$ concentrations proving the technologies polishing capabilities.

Other goals include optimization of cell materials capable of improving cell performance. Once cell materials are defined, cell experiments determining maximum removal capabilities and current efficiencies will be conducted.

Also, a model theoretically describing the preferred reduction of $H_2S$, the transport of $S^{2-}$, and the competing transport of $CO_2$ will be investigated. The model should identify the maximum current efficiency for $H_2S$ removal, depending on variables such as flow rate, temperature, current application, and the total cell potential.

## Introduction

The Electrochemical Membrane Separator (E.M.S.), the focus of experimental work, purges a fuel gas contaminated with $H_2S$. This is done by reducing the most electro-active species in the gas stream. In this case, $H_2S$ is reduced by the following:

$$H_2S + 2e^- \rightarrow H_2 + S^{2-} \tag{1}$$

A membrane which contains sulfide ions in a molten salt electrolyte will act to transport the ions across to the anode. If the membrane is impermeable to $H_2$ diffusion from the cathode side, an inert sweep gas can be used to carry the vaporous oxidized sulfur downstream to be condensed.

$$S^{2-} \rightarrow 1/2\ S_2 + 2e^- \tag{2}$$

Processes to remove $H_2S$ typically rely on low to ambient temperature adsorption, followed by sorbent regeneration and Claus plant treatment for conversion of $H_2S$ to a salable by-product, sulfur. Although effective, this type of removal is very process-intensive as well as energy-inefficient due to low temperature operation. Gasification streams generally range from $500^oC$ - $1000^oC$, requiring cooling before and reheating after process gas sweetening. Although these technologies have proven capable of meeting $H_2S$ levels required by MCFC, there are several disadvantages inherent to these processes[10,11].

Alternative high temperature methods are presently available, but process drawbacks including morphological changes in catalytic beds[12] or inefficient molten salt sorbent processes[13] negate savings incurred through energy efficient removal temperatures.

An electrochemical membrane separation system for removing $H_2S$ from coal gasification product streams is the subject of this investigation. The high operating temperature, flow-through design, and capability of selective $H_2S$ removal and direct production of elemental sulfur offered by this process provide several advantages over existing and developmental $H_2S$ removal technologies.
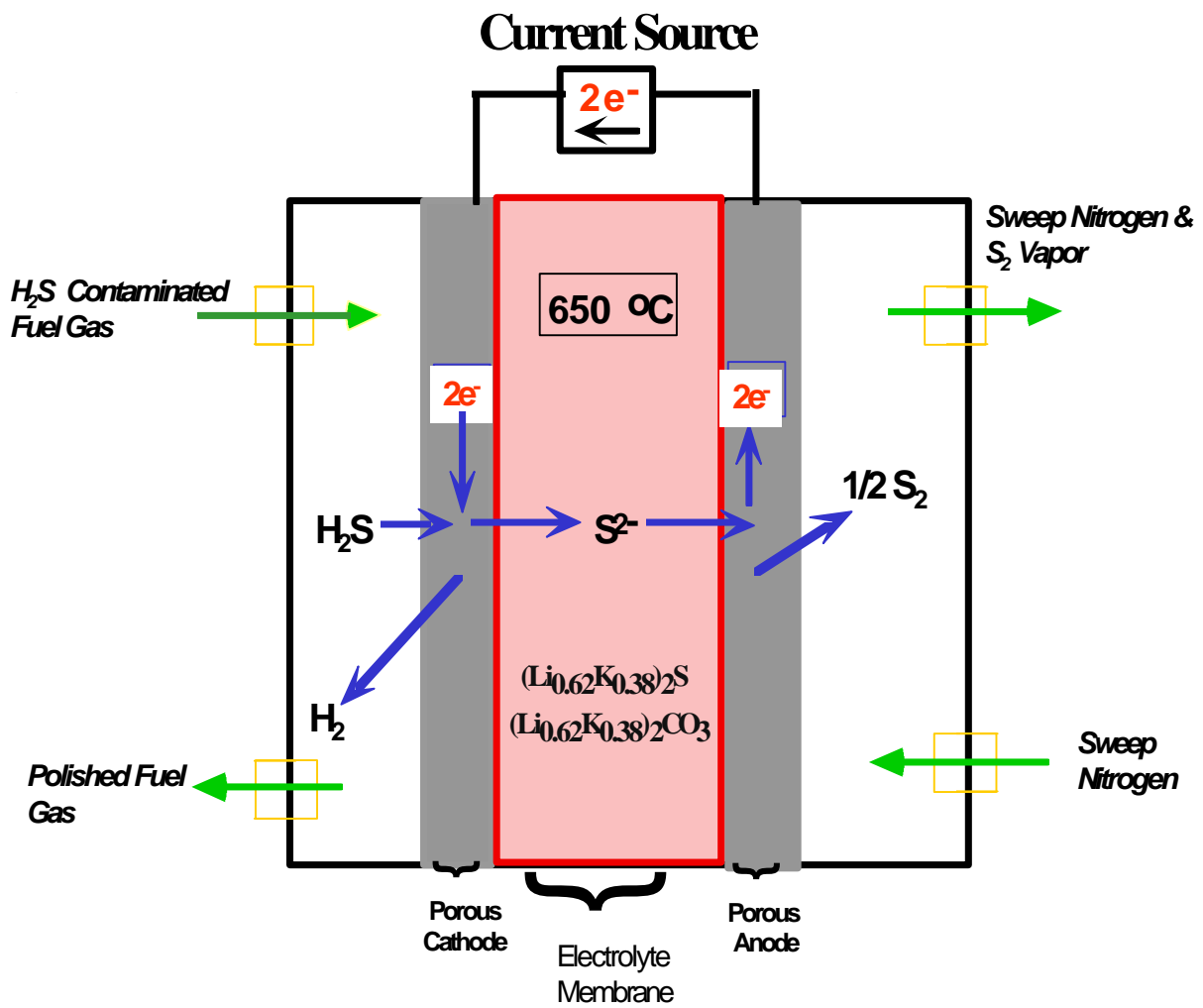
Current Source

2e⁻

Sweep Nitrogen &
S₂ Vapor

H₂S Contaminated
Fuel Gas

650 °C

2e⁻          2e⁻

1/2 S₂

H₂S →  → S²⁻ →

H₂

$(Li_{0.62}K_{0.38})_2S$
$(Li_{0.62}K_{0.38})_2CO_3$

Polished Fuel
Gas

Sweep
Nitrogen

Porous
Cathode

Electrolyte
Membrane

Porous
Anode

**Figure 1. Single-Cell View of the Electrochemical Membrane Separator**

## Results and Discussion

This quarter's research can be broken down into two distinct materials issues: the effectiveness of aluminum plasma coated cell housings in full cell runs, and the possibility of $LiCoO_2$ as an alternative cathode material . These will be discussed below in two separate sections. Table I summarizes all full cell runs carried out this quarter:

**Table I.  Full cell runs attempted this quarter.**

| Run # | Temp (°C) | Cathode | Anode | Membrane | Housings | Passivation |
|-------|-----------|---------|-------|----------|----------|-------------|
| 39 | 535 | Lithiated Ni, thickness: 0.70 mm | Lithiated Ni, thickness: 1.2 mm | Fabricated ZrO₂ | Stainless steel(316) | Exterior-Al plasma Wet seal-Al foil |
| 40 | 550 585 | Lithiated Ni, thickness: 0.81 mm | Lithiated Ni, thickness: 1.2 mm | Fabricated ZrO₂ | Stainless steel(316) | Exterior-Al plasma Wet seal-Al plasma |
| 41 | 580 593 | Lithiated Ni, thickness: 0.58 mm | Lithiated Ni, thickness: 1.2 mm | Fabricated ZrO₂ | Stainless steel (316) | Exterior-Al plasma Wet seal-Al plasma Al₂O₃ aerosol |
| 42 | 585 | Lithiated Ni, thickness: 1.2 mm | Lithiated Ni, thickness: 1.2 mm | Tape-casted ZrO₂ | Stainless steel (316) | Exterior-Al paint Wet seal-Al paint Al₂O₃ aerosol |
| 43 | 620 | LiCoO₂, thickness: | Lithiated Ni, thickness: | Fabricated | MACOR | No passivation |

**650**              0.98 mm              1.2 mm              ZrO$_2$

**680**

## Stainless steel cell housings

The primary thrust of this quarter's research focused on full cell EMS experiments utilizing passivated stainless steel cell housings. Best results (Run #40) were obtained with cell housings plasma coated with aluminum in order to passivate the exposed stainless steel.  The plasma coating was performed by Plasma Coatings, Inc.  In addition, an $Al_2O_3$ aerosol was applied to the cell housings in two runs.  All of these runs employed  pre-fabricated 85% porous nickel provided by ERC as the cathode and anode material.  Fabricated membranes purchased from Zircar Corporation were used in these full cell experiments.  Cell housings were plasma coated with aluminum in order to passivate the exposed stainless steel.  Temperatures for these runs ranged from 530 °C to 580 °C in order to avoid cathode dissolution due to the liquid eutectic formed between nickel and hydrogen sulfide above 600 °C.

The purpose of full cell runs was:  1.) test the electrochemical membrane separator's ability to transport $CO_3^{2-}$ ; 2.) test the electrochemical membrane separator's ability to remove $H_2S$; and 3.) study the effects of temperature on $H_2S$ removal.

## Carbonate Transport

Before the addition of $H_2S$ to the cell, it is necessary to evaluate the electrochemical membrane separator's ability to transport carbonate across the cell.  This is accomplished by $CO_2$ removal from the process gas (cathode coal syn-gas) (**3**):

$$CO_2 + H_2O + 2e^- \rightarrow H_2 + CO_3^{2-} \tag{3}$$
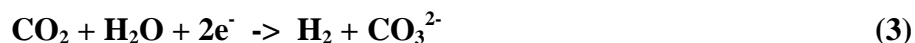
and anode $CO_2$ evolution due to carbonate oxidation (**4**):

$$CO_3^{2-} \rightarrow CO_2 + \frac{1}{2}O_2 + 2e^- \tag{4}$$

This is the first test performed during a full-cell run which displays the EMS cell's performance. Based on 2 Faraday's of charge transferred per mole of species reduced or oxidized, the actual carbon dioxide removed/produced can be compared to theoretical amounts. A current step method is utilized to determine the carbon dioxide removal, carbon dioxide production, as well as cell potential at varying applied currents. Run #39 failed due to poor cathode seals before any data could be collected, however, Runs 40-42 were all successful at carbonate transport and will be described in detail below.

Run #40

The EMS was tested for $CO_2$ removal at the cathode and $CO_2$ production at the anode. The cathode inlet flow rate was 195 cc/min while the cathode outlet flow rate was 115 cc/min. Meanwhile, the anode inlet flow rate was 191 cc/min with an outlet flow rate of 182 cc/min. The cathode inlet gas concentration before the water-gas shift reaction was 1.82 % $CO_2$, 4.60 % CO, 10.00 % $H_2O$, 13.81 % $H_2$, and balance $N_2$. A current step experiment was employed to determine $CO_2$ removal and production versus applied currents. Cathode $CO_2$ removal data is shown in Figure 2, while anode $CO_2$ production is shown in Figure 3.

Run #41

The EMS was tested for carbonate transport in the same manner as Run #41. Two cathode inlet flow rates were attempted. Stoichiometric $CO_2$ removal and production was demonstrated for a cathode inlet stream of 145 cc/min and outlet of 115 cc/min with corresponding anode inlet and outlet flow rates of 191 cc/min and 182 cc/min, respectively. The cathode gas concentrations were as follows (before water-gas shift reaction): 1.90 % $CO_2$, 4.77 % CO, 14.43 % $H_2$, 10.00 % $H_2O$, and balance $N_2$. $CO_2$ removal is demonstrated in Figure 4. Carbonate transport experiments were also run at a cathode inlet flow rate of 217 cc/min and resulting outlet flow rate of 154 cc/min. The anode flow rates remained the same. The cathode inlet gas concentrations in this case were: 2.09 % $CO_2$, 5.26 % CO, 15.88 % $H_2$, 10.00 % $H_2O$, and balance $N_2$. Cell potential data for this experiment is demonstrated in Figure 5.

Run #41

Like previous runs, carbonate transport was again demonstrated in this experiment. However, this experiment utilized a tape-cast membrane manufactured in this lab. Although thinner than the Zircar-manufactured membranes, the tape-cast membranes are very fragile and excess cell manipulation will cause cracking. The cathode inlet gas flow rate for carbonate transport experiments was 160 cc/min with an outlet flow rate of 97 cc/min. Meanwhile, the anode inlet flow rate was 147 cc/min, and the outlet flow rate was 133 cc/min. The cathode inlet gas concentrations before the water-gas shift reaction were: 1.67% $CO_2$, 4.20 % CO, 12.69% $H_2$, 10.00 % $H_2O$, and balance $N_2$. Figure 6 illustrates the effectiveness of $CO_2$ removal. However, stoichiometric $CO_2$ production was not achieved, as evidenced by Figure 7. This may be due to faulty seals which led to poor data collection. In addition, oxidation of carbonate at any exposed stainless steel anodic housing may have drained current from the desired reaction at the anode.

This parasitic reaction would drain current from the desired anodic reaction, thus anodic $CO_2$ production would be less than predicted.

All of these runs demonstrated effective carbonate transport. Moreover, applied cell potentials were within anticipated bounds. Therefore, $H_2S$ removal experiments were attempted in all cases.
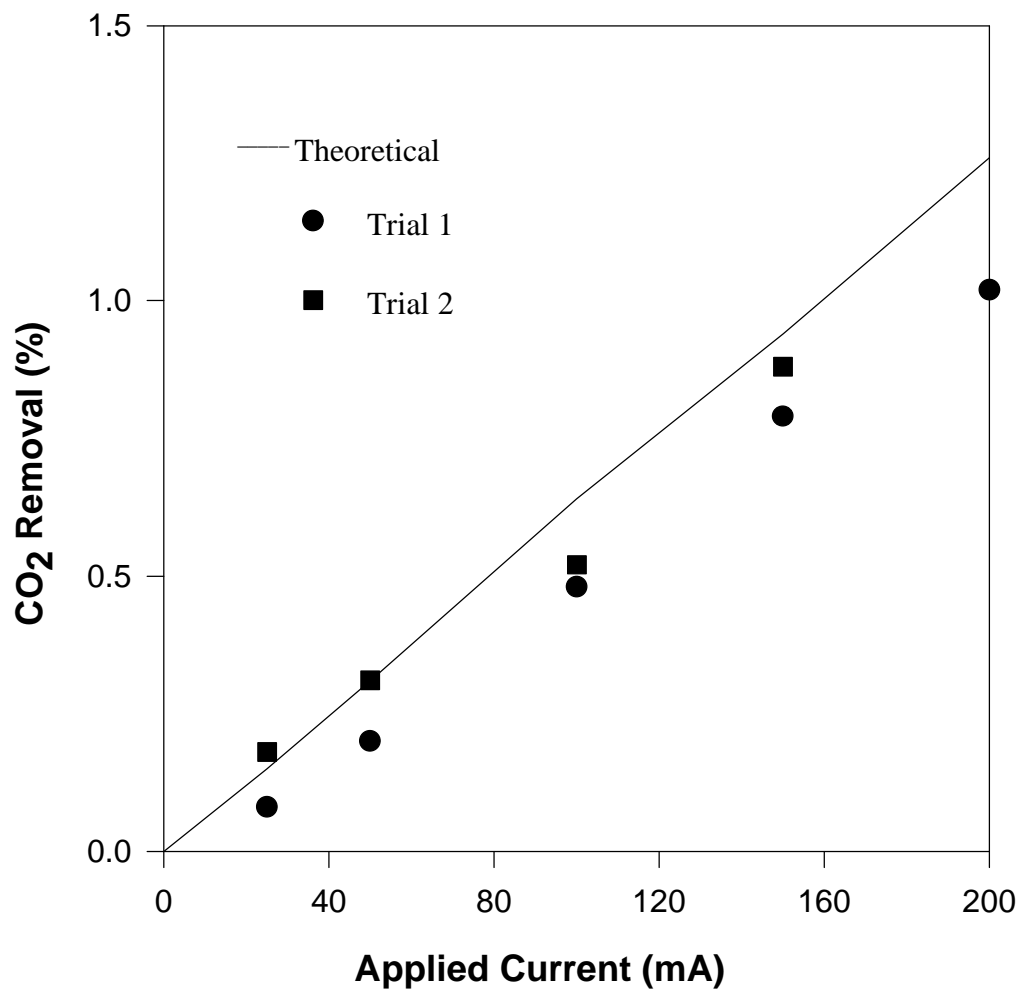
# CO$_2$ Removal vs. Applied Current



**Figure 2. Run #40. Carbonate Transport - CO$_2$ Removal vs. Applied Current**

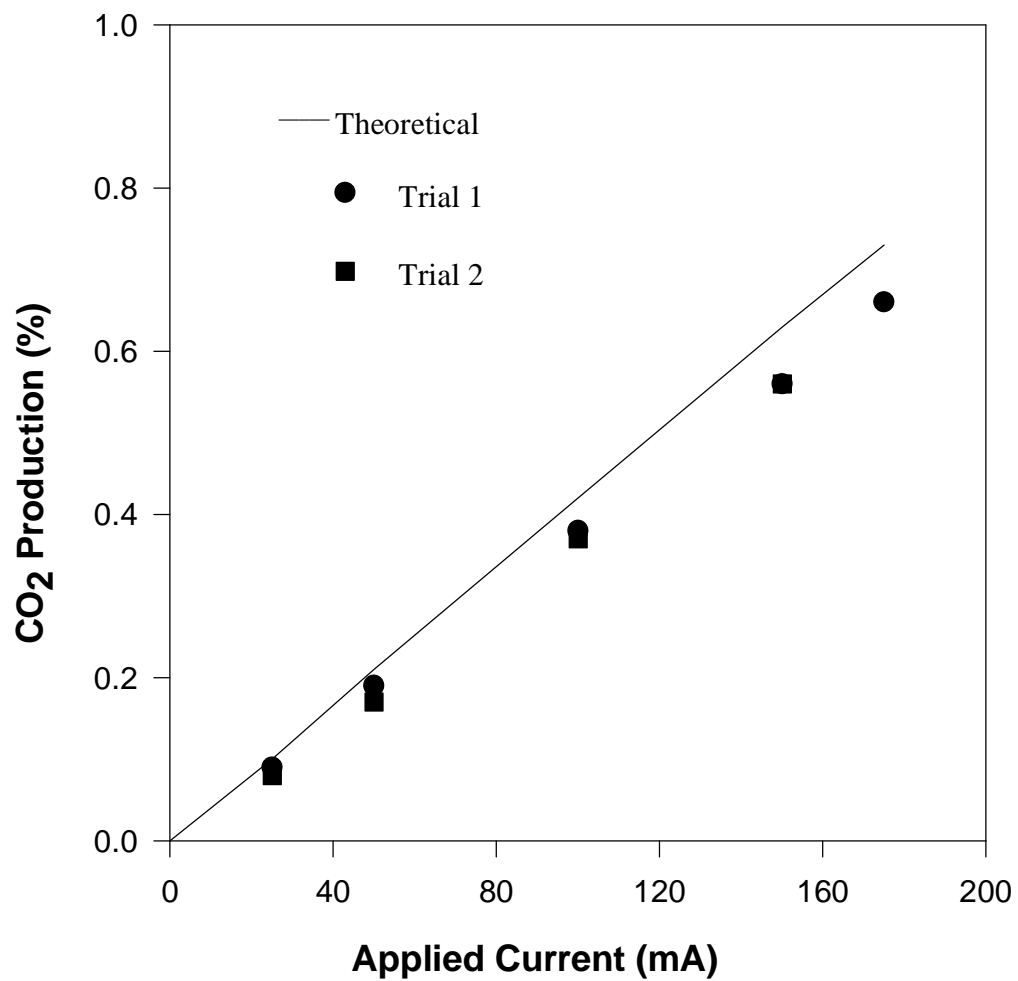# CO$_2$ Production vs. Applied Current



**Figure 3. Run #40. Carbonate transport - CO$_2$ Production vs. Applied Current**

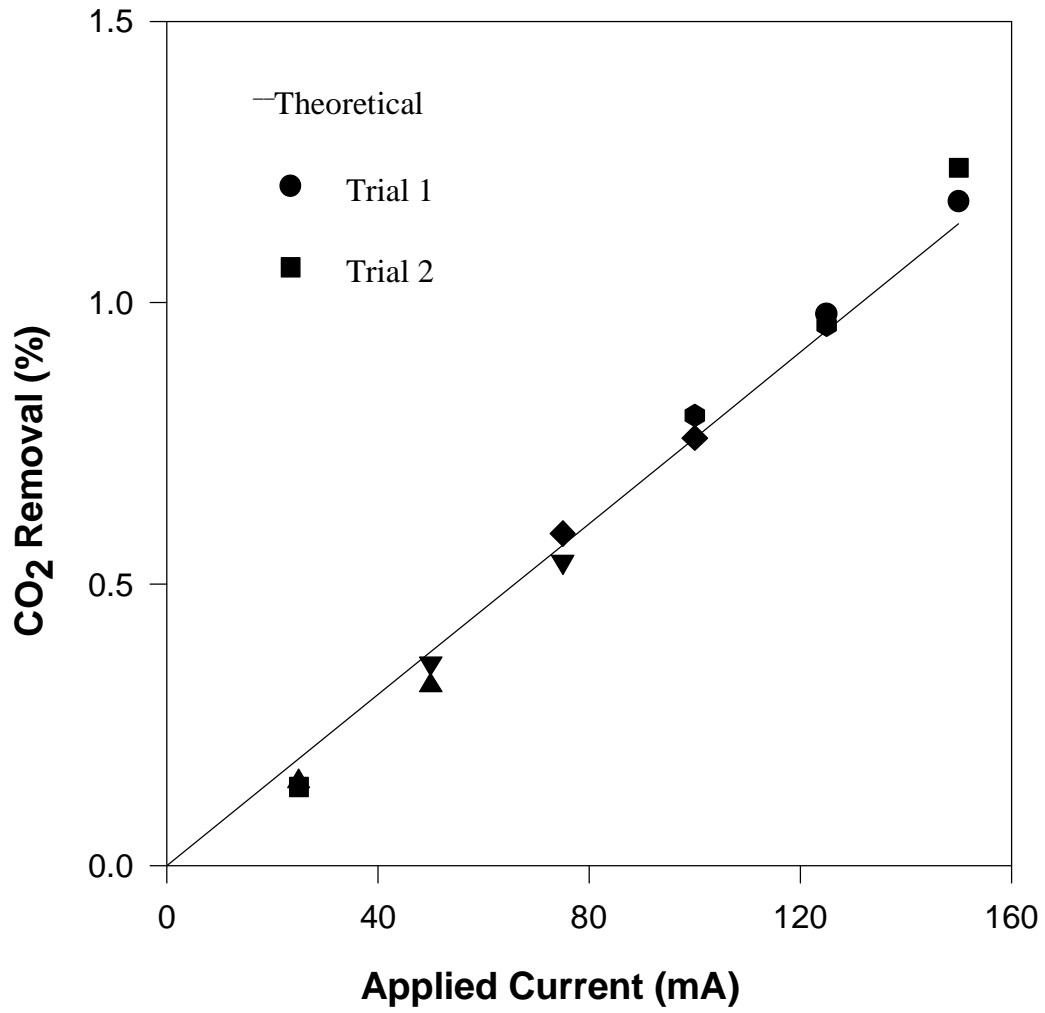# CO$_2$ Removal vs. Applied Current



**Figure 4. Run #41. Carbonate Transport - CO$_2$ Removal vs. Applied Current**
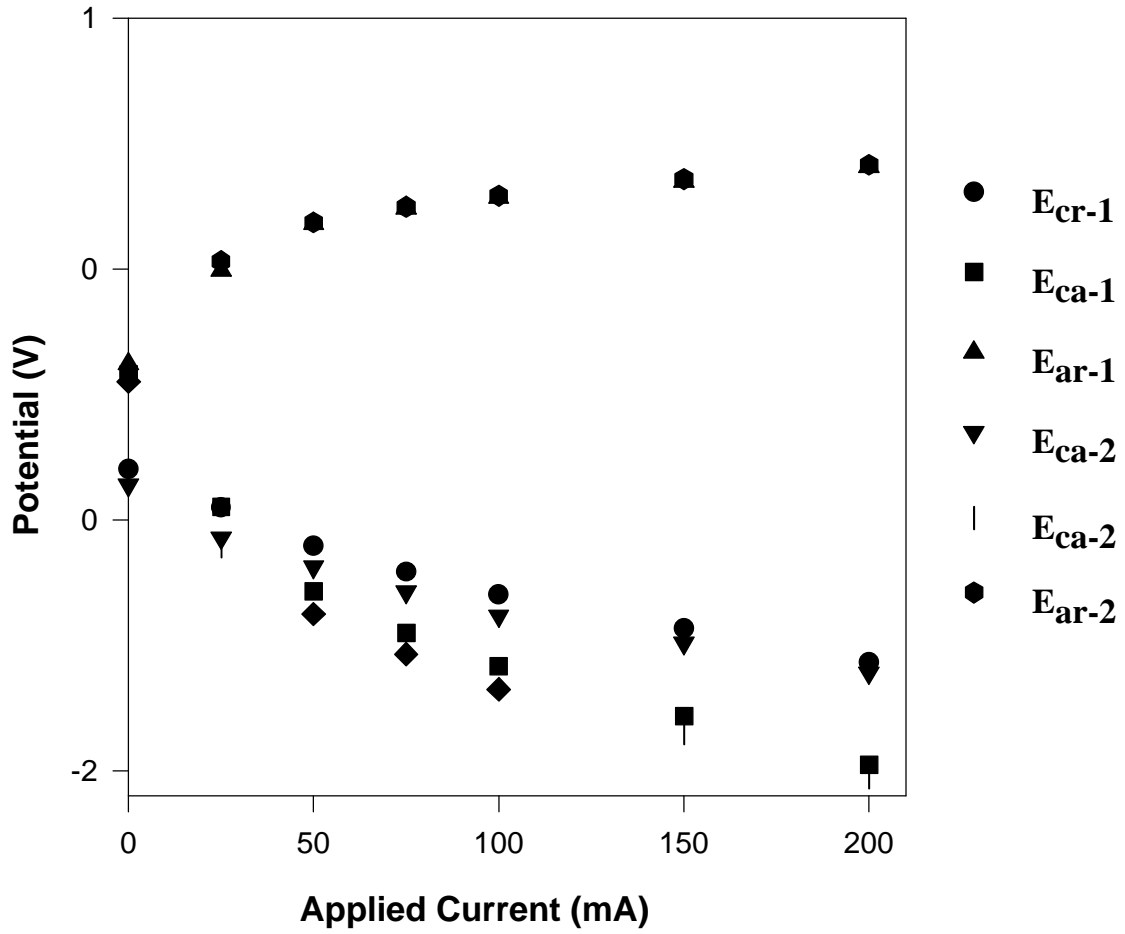
# Cell Potential vs. Applied Current



**Figure 5.  Run #41.  Carbonate Transport - Cell Potentials vs. Applied Current**
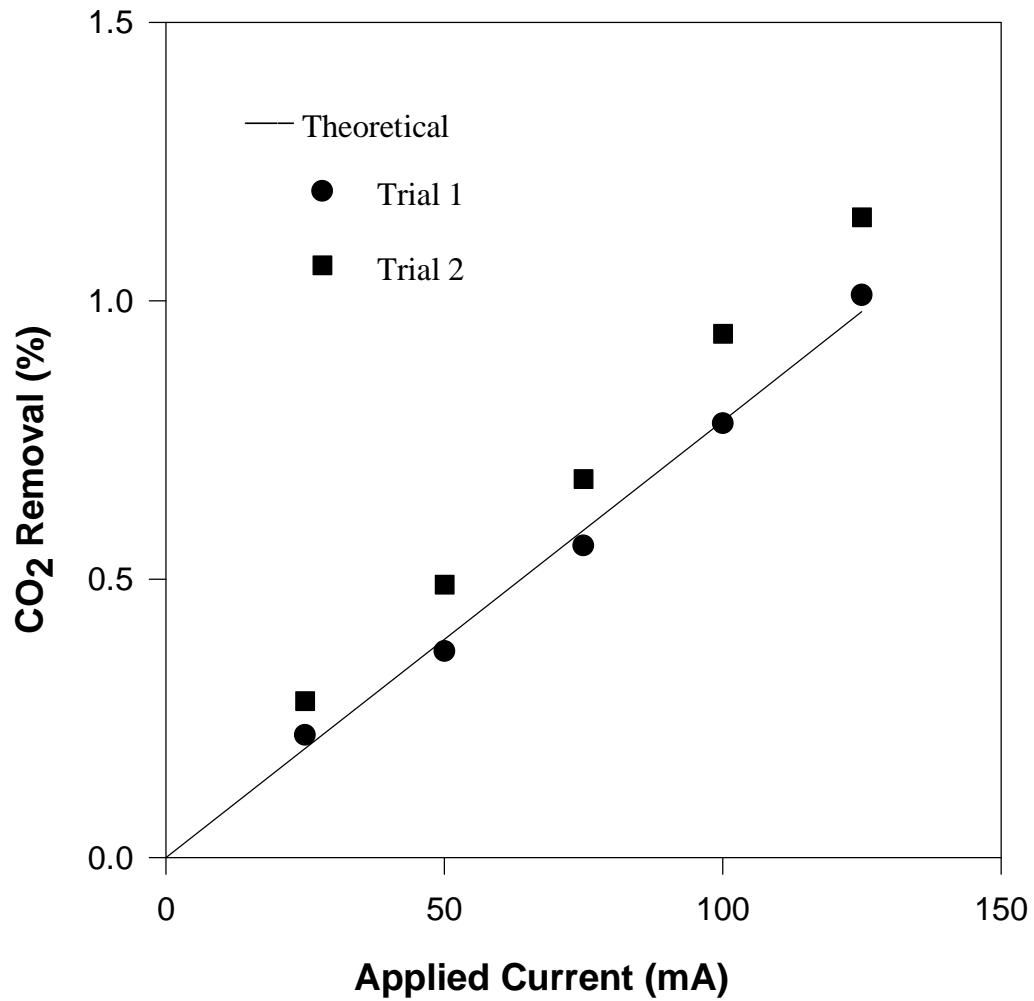
# CO$_2$ Removal vs. Applied Current



**Figure 6. Run #42. Carbonate Transport - CO$_2$ Removal vs. Applied Current**

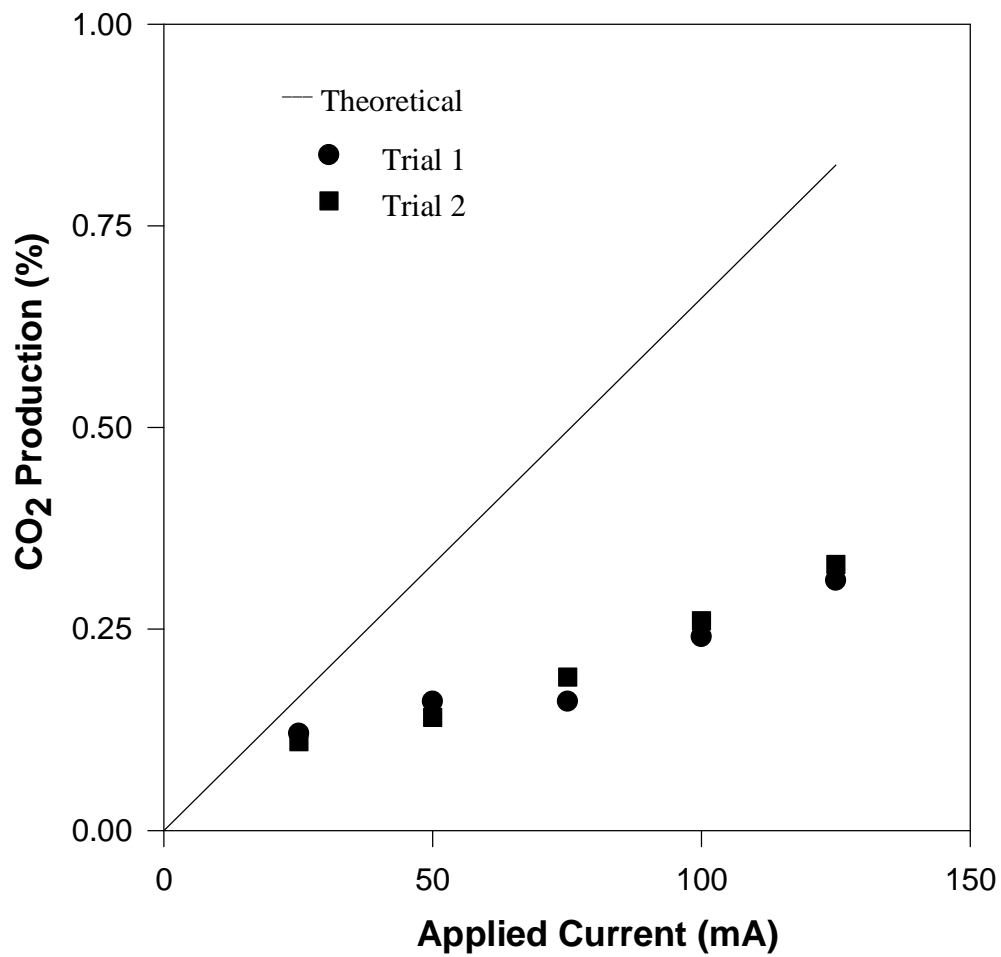# CO$_2$ Production vs. Applied Current



**Figure 7.  Run #42.  Carbonate Transport - CO$_2$ Production vs. Applied Current**

## Removal of H₂S from Sour Coal Gas

Once carbonate transport across the cell was demonstrated, $H_2S$ was added to the process syn-gas. The process gas was equilibrated by the following two reactions:

$$H_2 + CO_2 \Leftrightarrow H_2O + CO \qquad\qquad (5)$$

$$H_2S + CO \Leftrightarrow H_2 + COS \qquad\qquad (6)$$

via a stainless steel shift reactor before entering the cell housing. Once process gases entered the cell housings, they equilibrated with the molten electrolyte by:

$$(Li_{0.68}K_{0.32})_2CO_3 + H_2S \Leftrightarrow (Li_{0.68}K_{0.32})_2S + CO_2 + H_2O \qquad (7)$$

which creates a conversion of carbonate ions to sulfide ions depending on the concentration of $H_2S$ in contact with the electrolyte as well as the temperature of the cell. Increased temperatures result in higher molten sulfide concentrations which facilitate sulfide oxidation. Typically, at least twenty-four hours is necessary for this reaction to reach equilibrium.

The goal of full-cell experiments is to validate the removal capabilities of the EMS system while maintaining economically feasible current efficiencies (high current efficiencies at high inlet $H_2S$ concentrations). $H_2S$ current efficiency is calculated by:

$$\eta_{H_2S} = \frac{\% \, H_2S \, Removal_{actual}}{\% \, H_2S \, Removal_{theoretical}} \qquad\qquad (8)$$

which represents the ratio of H$_2$S actually removed to the amount that should be removed at a

specified applied current.  The following equation calculates the amount of $H_2S$ removed from the process syn-gas:

$$\% \, H_2S \, Removal = \frac{Inlet \, H_2S - Outlet \, H_2S_{(I_{app})}}{Inlet \, H_2S} \quad x100 \qquad (9)$$

All three runs with passivated stainless steel cell housings were tested for $H_2S$ removal and will be discussed below.

<u>Run #40</u>

Successful $H_2S$ removal was observed at three different flow conditions ranging from flow rates of 120 to 324 cc/min, and inlet $H_2S$ concentrations between 3000 ppm and 4000 ppm. These different conditions will be referred to as 40a, 40b, and 40c.  All runs were performed at the reaction temperature of 585 °C.  In addition, the anode flow rate for all subruns was 120 cc/min.  Run 40a  had a cathode inlet flow rate of 195 cc/min. The process gases equilibrated to: 3.81 % $CO_2$, 2.33 % CO, 7.94 % $H_2O$, 15.32 % $H_2$, 3122 ppm $H_2S$, 10 ppm COS, and  balance $N_2$. The molten salt equilibrium concentrations was estimated at 90.9 % $M_2CO_3$ and 9.1 % $M_2S$, where M represents the lithium/potassium eutectic.  The gas phase limiting current density was estimated at 36.2 mA/cm$^2$ while the membrane limiting current density was estimated at 88.2 mA/cm$^2$.  With an electrode area of 7.92 cm$^2$, the limiting current density for these conditions is 287 mA.  Applied current approaching this level will result in severe mass transfer limitations.

Run 40b had an increased flow rate of 324 cc/min with similar $H_2S$ inlet conditions (~3000 ppm $H_2S$).  The cathode inlet gas was estimated as follows (after water-gas shift reaction): 3.85

% $CO_2$, 2.39 % CO, 7.93 % $H_2O$, 15.55 % $H_2$, 2873 ppm $H_2S$, 29 ppm COS, and balance $N_2$. Limiting current densities in the gas phase and membrane were estimated at 33.3 mA/cm$^2$ and 88.2 mA/cm$^2$, respectively. Molten salt equilibrium was estimated at 91.3 % $M_2CO_3$ and 8.7 % $M_2S$.

The last set of conditions (Run 40c) had a decreased flow rate of 120 cc/min but an increased inlet $H_2S$ concentration of 3950 ppm. The concentrations of the gas entering the cell was estimated at: 4.19 % $CO_2$, 2.39 % CO, 7.93 % $H_2O$, 15.55 % $H_2$, 2873 ppm $H_2S$, 29 ppm COS, and balance $N_2$. Limiting current densities in the gas phase and membrane for this run were estimated at 45.2 mA/cm$^2$ and 99.9 mA/cm$^2$, respectively. The equilibrium molten salt composition was estimated at 89.3 % $M_2CO_3$ and 10.7 % $M_2S$.

Like the carbonate transport experiments, a current step was applied to determine the $H_2S$ outlet levels, % $H_2S$ removal, current efficiency, and the potential profile versus applied current. Figure 8 demonstrates that $H_2S$ outlet levels fall with increasing cell current for all 3 of the subruns. Figure 9 illustrates the $H_2S$ removal percent as a function of applied current and Figure 10 shows the resulting current efficiencies for the three subruns. Figure 11 displays the relationship between cell potential and applied current for Run #40b. It should be noted that internal resistance ranged between 3 and 3.5 ohms during the entire experiment. Run #40 was eventually stopped due to cathode clogging by excess electrolyte. This run was ended after 13 days.
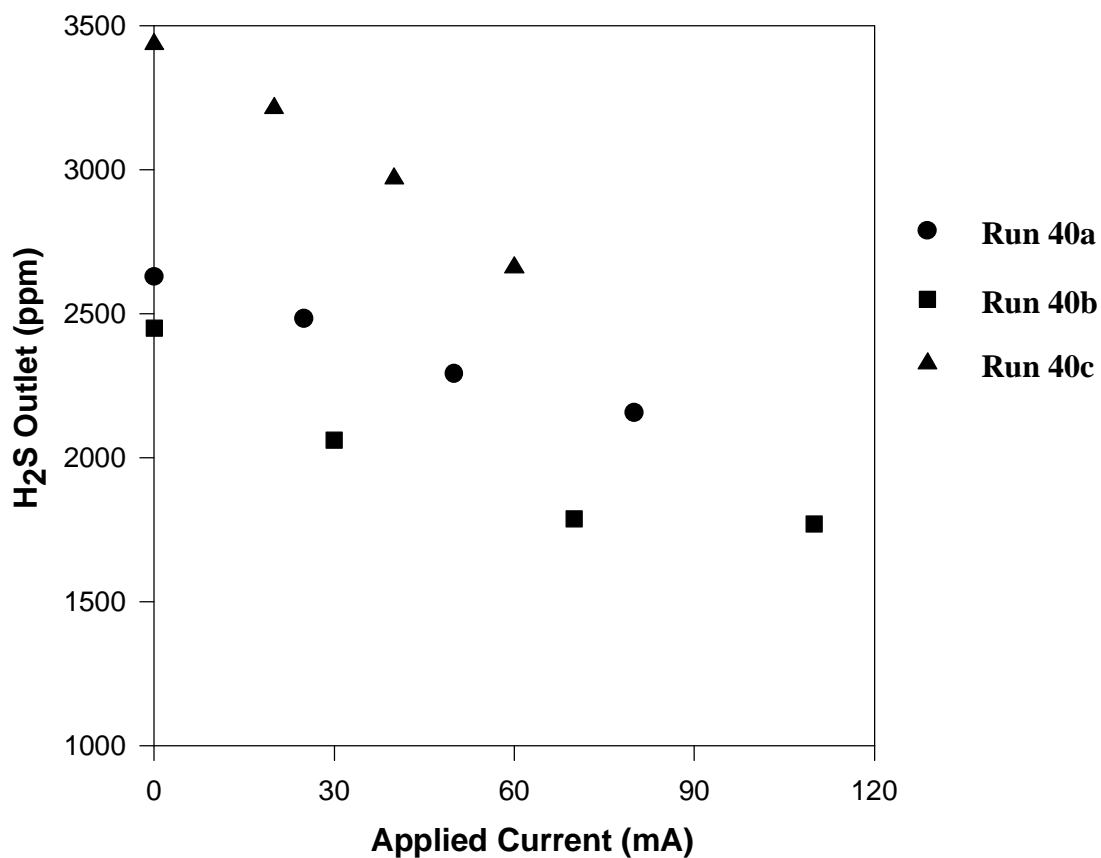
# H₂S Outlet vs. Applied Current



**Figure 8.  Run #40.  Outlet H₂S versus Applied Current**
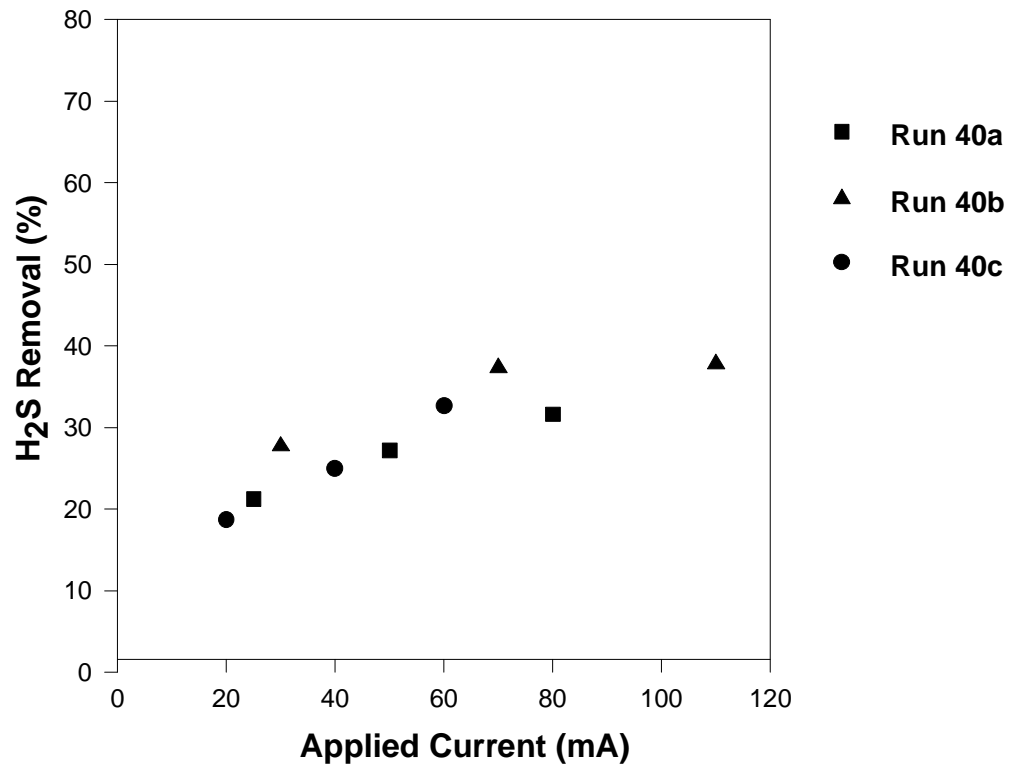
**H$_2$S Removal versus Applied Current**

**Figure 9.  Run #40.  H$_2$S Removal vs. Applied Current**

**Current Efficiency vs. Applied Current**

Run 40a
Run 40b
Run 40c

Current Efficiency (%)
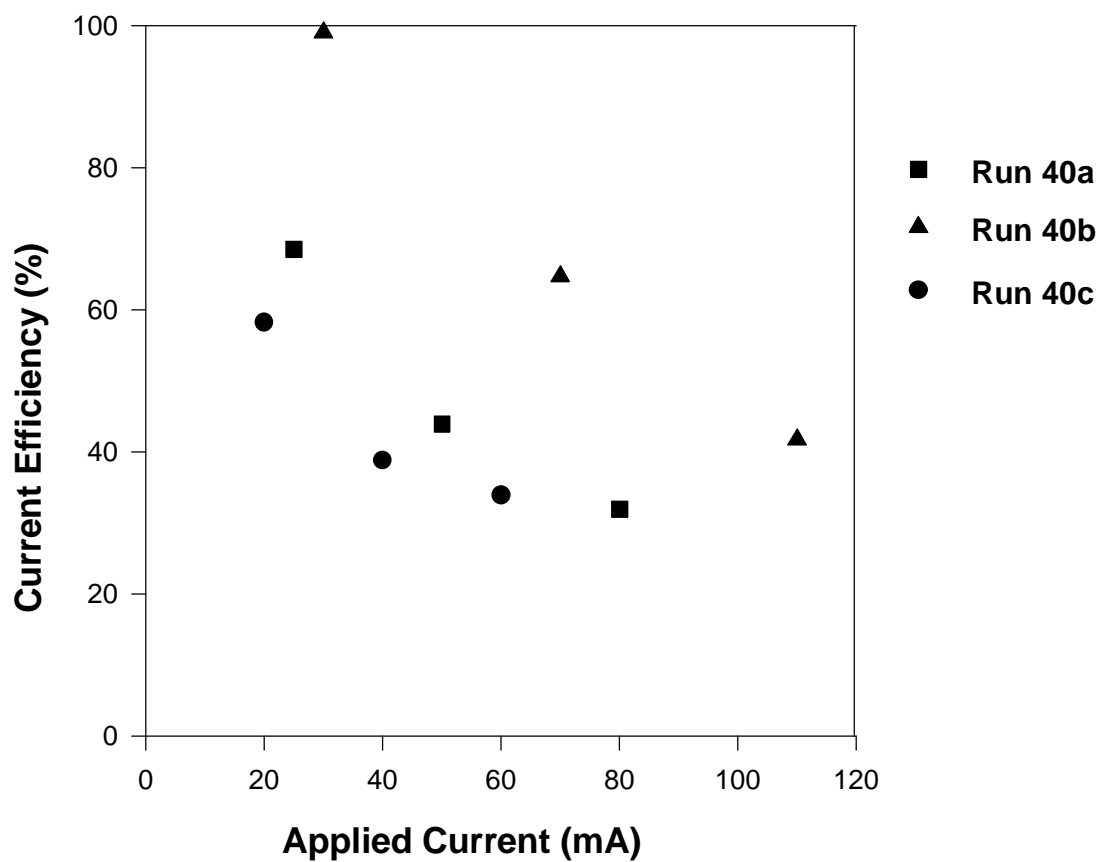
Applied Current (mA)

**Figure 10.  Run #40.  Current Efficiency vs. Applied Current**

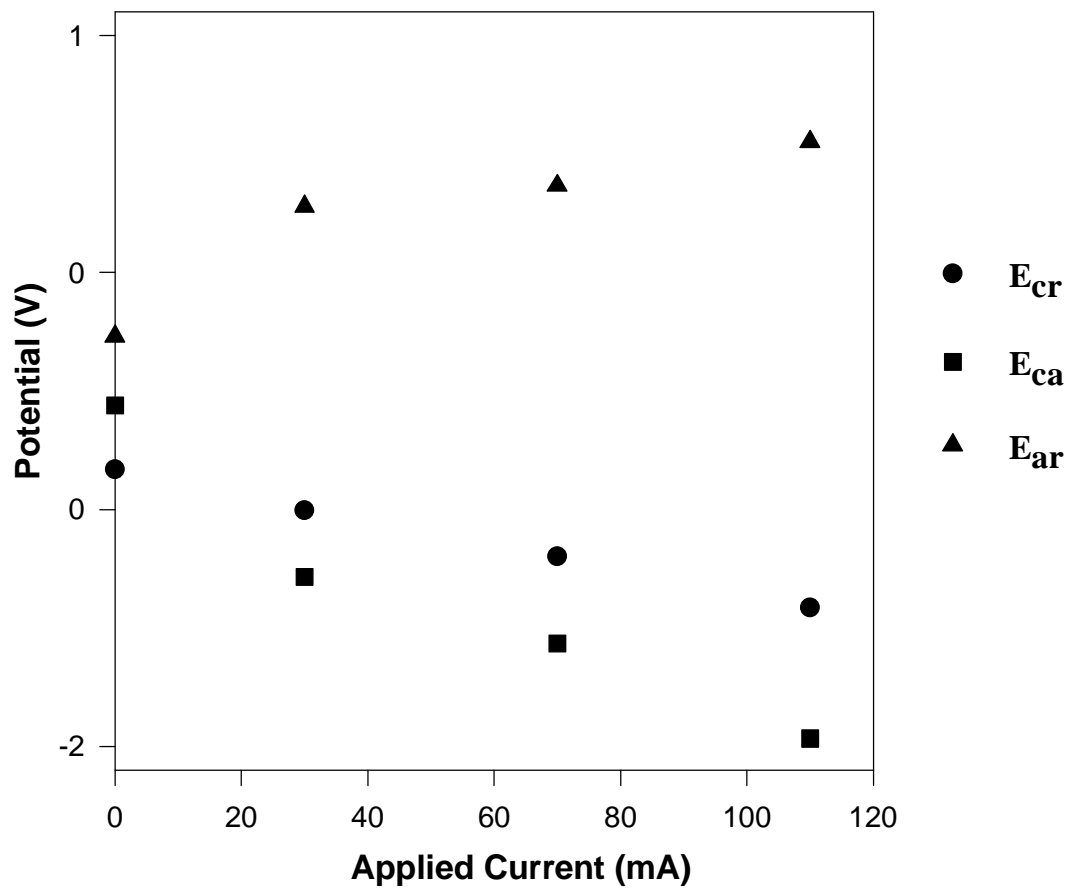**Cell Potential vs. Applied Current**



**Figure 11. Run #40b. Cell Potentials vs. Applied Current**

Run #41

Attempts at $H_2S$ removal were unsuccessful for this run. In addition to the aluminum plasma coating of the stainless steel cell housings, aerosol $Al_2O_3$ from Alfa-Aesar was applied on top of the aluminum. Carbonate transport was observed, however, attempts at $H_2S$ removal were unsuccessful. The run was terminated after 7 days.

Run #42

$H_2S$ was applied to the cathode inlet gas during this fun, but $H_2$ crossover led to poor results. The tape-cast membrane was too thin to inhibit gas cross-over. Excessive cell manipulation led to membrane cracking. In addition, cathode flow was hindered by excess electrolyte in the cathode gas flow chamber. The run was concluded after 11 days.

Discussion

The positive results obtained from Run #40 demonstrate that cell housing passivation is necessary to achieve $H_2S$ removal when using stainless steel cell housings. Without a passivation layer, any exposed carbonate in contact with the conductive anodic cell housing would be oxidized. This process promotes carbonate transport in the EMS, rather than sulfide transport which is necessary for $H_2S$ removal. Figures 8-10 show that the EMS achieved $H_2S$ removal for different conditions. In all cases, $H_2S$ removal increased as applied current was increased, which is expected. However, the current efficiencies dropped with increasing current.

Two possible explanations for this result will be discussed in detail below.

The equilibrium between the process gases and the molten electrolyte which is shown in equation (**7**) is very much dependent on temperature. At a temperature of 580 °C, the reaction as

written is non-spontaneous with an equilibrium constant of 0.419. However, at 627 °C, the equilibrium is spontaneous as written with an equilibrium constant of 1.108. Molten sulfide formation is desired since it must be oxidized at the anode to promote $H_2S$ removal. $H_2S$ removal was attempted at a temperature of 550 °C, but this was unsuccessful. Once temperature was increased to 585 °C, $H_2S$ removal was observed. Thus, cell temperatures must be high enough to insure that there is an adequate amount of $M_2S$ in the electrolyte. If not, the $H_2S$ removal process is mass-transfer limited at the anode due to lack of sulfide ions at the electrode surface for oxidation. Perhaps even greater $H_2S$ removal would be observed at even higher run cell temperatures. The desired operating temperature of the EMS is 650 °C. However, the use of nickel as the cathode limits reaction temperatures to 585 °C due to liquid $Ni_3S_2$ formation at temperatures above 600 °C.

Lower than desired current efficiencies could also be a result of poor electrolyte distribution. At the start of all cell runs, a pre-pressed disk of $(Li/K)_2CO_3$ is placed above the zirconia membrane. This melts at 492 °C and saturates the membrane as the temperature is increased to the operating temperature. However, during the cell run, the membrane and electrodes are depleted of electrolyte due to evaporation and corrosion. Thus, excess electrolyte must be provided to the EMS. This is difficult to accomplish at high temperatures. Typically, a crucible of electrolyte is placed beside the furnace and allowed to melt. When internal resistance is substantial, liquid electrolyte is added to the corner of the cathodic cell housing where a hole has been drilled through to allow the molten carbonate to reach the membrane. Post-mortem analysis of the cell housing has shown that too much electrolyte was added. $K_2SO_4$ (as evidenced by X-ray diffraction) was found in the cathode well after all stainless steel cell runs this quarter.

The formation of $K_2SO_4$, discussed in the previous quarterly report, is due to $K_2S$ reacting with oxygen. The fact that the electrode wells are flooded can lead us to conclude that the cathode itself is probably flooded. The proper mechanism for $H_2S$ removal calls for cathode pores being "wetted" with electrolyte so that $H_2S$ can be in simultaneous contact with the cathode and the electrolyte. However, flooded pores decrease the amount of sites available for $H_2S$ reduction. $CO_2$ and $H_2O$, which are present on the percent level, are also available for reduction at the remaining reduction sites which are not flooded. Since they are more abundant than $H_2S$, they are more likely to be reduced, thus lowering $H_2S$ current efficiency. Thus, electrolyte management must be stressed during these experiments to ensure that the cathode pores are not flooded.

Cathode thickness was also decreased for all cell runs this quarter. This was performed mainly to allow for cathode expansion when the nickel cathode was in the presence of $H_2S$ resulting in $Ni_3S_2$. A thinner electrode would allow extra room to hopefully avoid expansion into the cathode gas flow chamber. $K_2SO_4$ found in the flow chamber after the experiments indicated that the cathode had not expanded into the flow chamber, but rather too much electrolyte had been added. Nonetheless, thinner electrodes lower internal resistance and thus are preferred.

The distinguishing materials factor between Runs #41 and #42 was the $Al_2O_3$ aerosol which was sprayed onto the aluminum passivation layer of the stainless steel cell housings in Run #42. Both runs exhibited stoichiometric carbonate transport, but only Run #41 was successful in $H_2S$ removal. It still cannot be determined at this point whether this is due to the $Al_2O_3$ aerosol. More experiments will be conducted to try to optimize the aluminum passivation layer.

$H_2S$ removal has been achieved with stainless steel cell housings in the past, but these were of polishing $H_2S$ levels ($< 100$ ppm)[14]. These are the first positive results for passivated

stainless steel housings that have been achieved with sour gas streams at 580 °C with a nickel cathode. Over 90 % $H_2S$ removal at greater than 90 % current efficiency of sour gas streams has been achieved with MACOR cell housings at variable flow rates in the past[15]. However, MACOR is not suitable to an industrial environment. Therefore, further attempts with stainless steel cell housings will be attempted, hopefully matching the results achieved with MACOR cell housings.

## Alternative Cathode Material - LiCoO$_2$

An alternative cathode material to nickel which can operate effectively at 650 °C must be discovered in order to enhance the EMS. One such candidate is LiCoO$_2$. LiCoO$_2$ has been utilized as a novel cathode material for the molten carbonate fuel cell[16,17,18]. Tennakoon et al. used the Pechini method to form LiCoO$_2$[17]. Lagergren et al. utilized the more simplistic solid-state reaction between Li$_2$CO$_3$ and CoCO$_3$[18]. The common reagents and ease of this reaction prompted us to attempt this reaction to form LiCoO$_2$. Successful synthesis led to electrode fabrication by dry pressing followed by a full cell run employing LiCoO$_2$ as the cathode material.

### LiCoO$_2$ Synthesis

Lithium carbonate and cobalt carbonate react in the presence of air at high temperatures to form lithium cobalt oxide as shown below:

$$\mathbf{Li_2Co_3 \;+\; 2CoCO_3 \;+\; \frac{1}{2}O_2 \;\rightarrow\; 2LiCoO_2 \;+\; 3CO_2} \qquad (10)$$
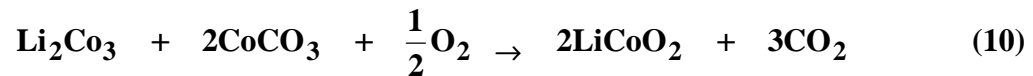
Li$_2$CO$_3$ and CoCO$_3$ were ball-milled with a weight ratio of 1:3 in air. This ratio corresponds to a 7 % excess of Li which insures that no Co$_3$O$_4$ would be formed. After milling for 24 hours, the mixture was ready for calcination. Literature suggested that optimal temperature for calcination was 650 °C.[18] The mixed powder was placed in an alumina crucible and placed in a Lindberg furnace for 6 hours at 650 °C, with a 3 °C/min ramp to and from the calcination temperature. After the reaction was complete, X-ray diffraction was performed to insure that the synthesis was successful. Figure 12 compares the X-ray diffraction pattern of our sample to the library index for LiCoO$_2$. The sample pattern matched the LiCoO$_2$ library reference pattern, thus indicating a successful synthesis. Moreover, no Co$_3$O$_4$ was evident in our sample. Therefore,

Figure 12. LiCoO$_2$ powder X-Ray Diffraction



Sample: licoo2   File: LICO2.DI                           3-SEP-97   14:59

x10$^2$
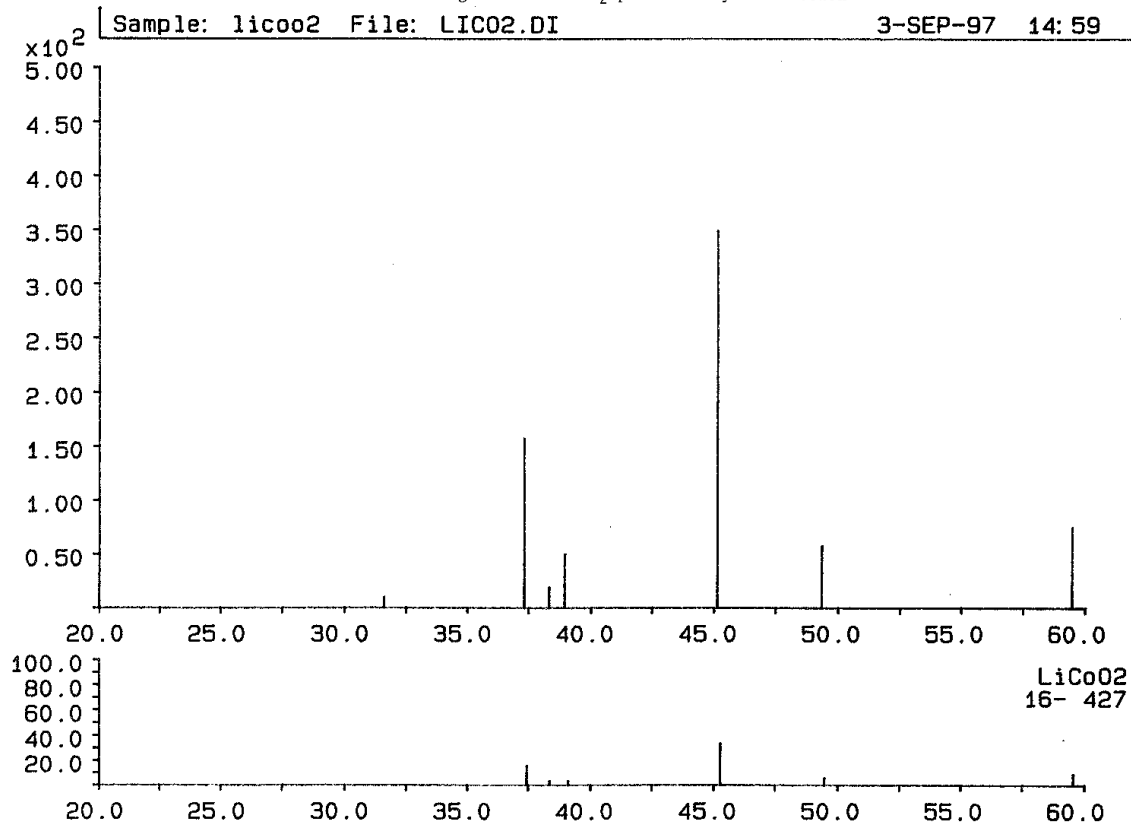
LiCoO2
16- 427

further tests monitoring $LiCoO_2$ stability in sulfurizing conditions could be conducted.

Stability of $LiCoO_2$ in a sulfurizing environment

MCFC literature did not study the effects of a sulfur environment $LiCoO_2$ since they hope to operate in a sulfur-free environment. However, since our electrodes must operate in a strong sulfurizing environment, preliminary tests were performed to determine the effects. 0.8g of $LiCoO_2$ was placed in an alumina closed-ended tube and subject to a gas stream of 2500 ppm $H_2S$ in nitrogen at 650 °C for 48 hours. X-ray diffraction of the resulting powder is shown in Figure 13. It is fairly obvious that $LiCoO_2$ no longer was present, but peak identification utilizing the Hanawalt index was unsuccessful. $LiCoS_2$, which seems to be the most probable resulting compound of this experiment, is not in the X-ray diffraction index. In fact, a literature search of our sample for any possible peak identification was unsuccessful.

This experiment was completed in the absence of a carbonate environment and typical fuel gas constituents($CO_2$, $H_2O$, and CO), which are present in full-cell runs. This environment would probably favor $LiCoO_2$. Therefore, future tests need to be done which mimic actual EMS full-cell run conditions.

Electrode Fabrication

The most convenient method of electrode fabrication was dry pressing followed by sintering, since the necessary materials were all available. Giorgi et al. synthesized $LiCoO_2$ electrodes[16] via dry pressing, so a similar method was adopted. The success of electrode fabrication by Giorgi et al. depended on the amount of poreformer added to pure $LiCoO_2$ before pressing as well as the sintering conditions (time, temperature, atmosphere). Since this work had

Figure 13. Result of sulfurizing environment on $LiCoO_2$

Figure 13. Result of sulfurizing environment on $LiCoO_2$

Sample: licoo2    File: LICO5.DI                    28-OCT-97    19:31

LiCoO2
16- 427
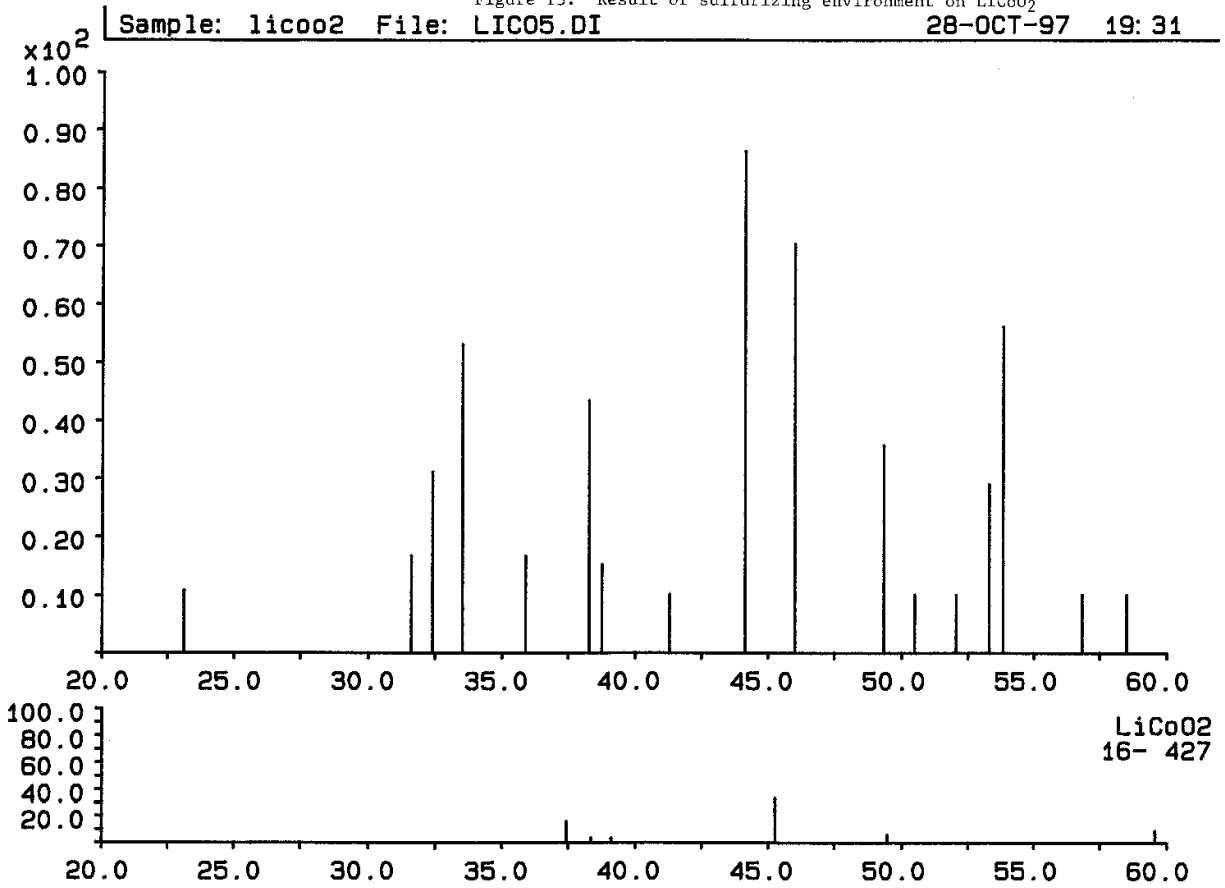
never been attempted in this laboratory, we utilized conditions that were favorable for Giorgi et al. and then used trial and error from that point.

Disks were pressed in either a 1.25" or 1.75" die. Poreformers were also added in various amounts. Approximately 2.0g of powder was loaded into the 1.25" die and 4-4.3g of powder was loaded into the 1.75" die. Approximately 9000 psig was applied to the die in all cases. The resulting circular disk was then transferred to the Lindberg furnace for sintering. Two sintering programs were used: (A)  1 °C /min to 350 °C for 4h, 1 °C/min to 600 °C for 4 h, 1 °C/min to 850 °C for 5h, and 1 °C/min to 25 °C or (B) 1 °C/min to 500 °C for 4h, 1 °C/min to 850 °C for 5h, and 2 °C/min to 25 °C. Table 2 provides a tabular summary of fabrication conditions. More work will need to be performed in order to determine proper conditions for sufficient electrode fabrication. Nevertheless, Trial 3 fabrication yielded a 1.75" circular disk which could be sanded down and used in a full cell run. The disk had a geometrically-derived porosity of approximately 82%, which is the necessary porosity to assure proper gas distribution. The thickness was 0.1 cm and the weight of the electrode was 2.815g. Although the disk had a slight crack of 0.3 cm, it was still utilized in a full-cell EMS run.

**Table 2.  LiCoO$_2$ Electrode Fabrication Conditions**

| Trial | Disk Size | Wt % Poreformer | Sintering Program | Fabrication Result |
|-------|-----------|-----------------|-------------------|--------------------|
| 1 | 1.25" | 25% | A | Poor, cracked |
| 2 | 1.75" | 25% | B | Poor, cracked |
| 3 | 1.75",1.25" | 5% | B | Good, slight cracks |
| 4 | 1.75" | 5%,4% | B | Fair |

Conditions for Full Cell Run

Run #43 was performed with MACOR cell housings in order to study the $LiCoO_2$ electrode without having to account for the effects of stainless steel cell housings. The temperature for this experiment ranged from 620 °C to 680 °C, well above the operating temperature when utilizing Ni cathodes. Gold wires were fed through the alumina gas flow tubes in order to carry the current to the electrodes. The gold wires ended as a current collector, where they were in contact with the electrode interface.

Carbonate Transport

The EMS was tested for $CO_2$ removal at the cathode and $CO_2$ production at the anode. In addition, potentials were recorded versus stepwise applied current. The temperature for this set of experiments was 650 °C. The cathode inlet flow rate was 137 cc/min while the cathode outlet flow was approximately 60 cc/min. The anode inlet and outlet flow rates were 114 cc/min and 62 cc/min, respectively. For carbonate transport experiments, the cathode inlet gas concentration after the water-gas shift reaction was 2.58 % $CO_2$, 6.49% CO, 10.00 % $H_2O$, 19.60 % $H_2$, and balance $N_2$. $CO_2$ removal data is displayed in Figure 14, while Figure 15 illustrates $CO_2$ production data. Figure 16 shows cell potential data versus stepwise applied current.

As can be seen from Figure 14, $LiCoO_2$ functions well as the cathode of the EMS. Stoichiometric $CO_2$ removal was achieved for a stepwise applied current up to 250 mA. Figure 15 shows that $CO_2$ was produced at the anode, although not stoichiometrically. This may be due to variable process anode gas seals. Figure 16 demonstrates that our cell is operating within anticipated cell voltages - and this figure is not compensated for internal resistance of the cell which ranged from 4 to 4.3 ohms. These results are very positive, especially considering that

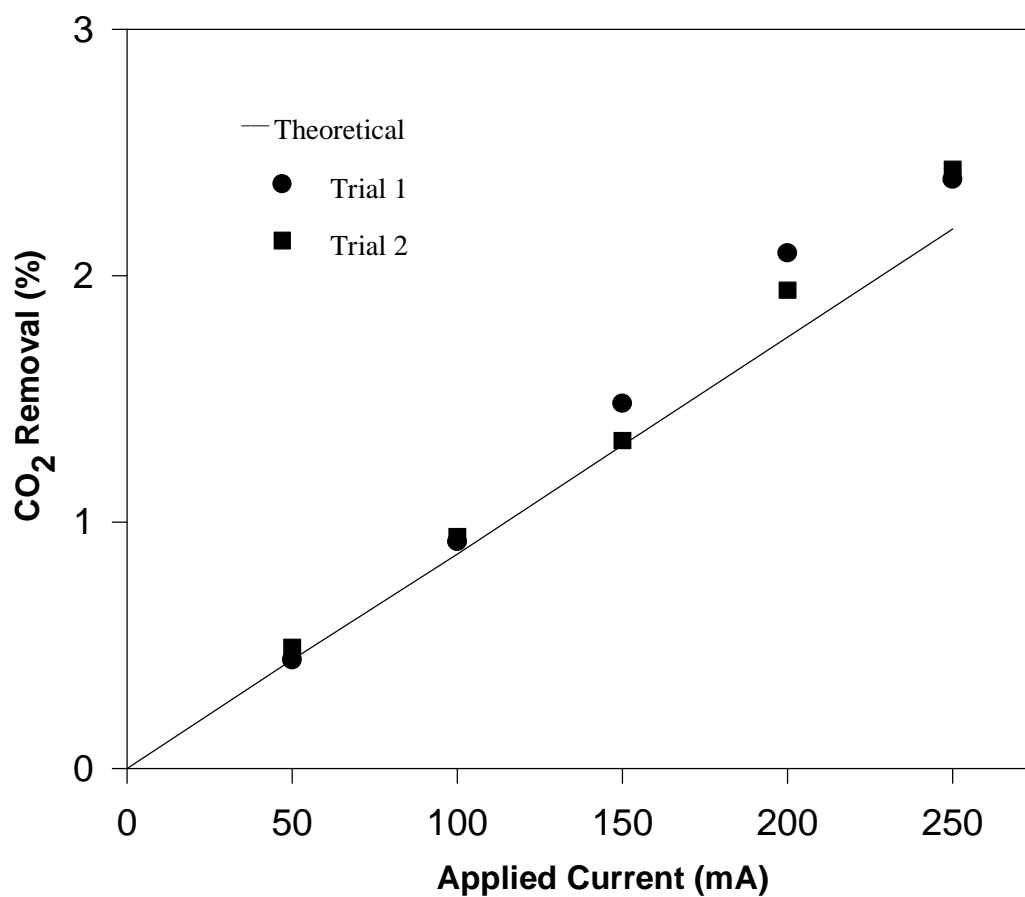**LiCoO$_2$ (as Cathode) Achieved Stoichiometric Removal of CO$_2$**



**Figure 14.  Run #43.  Carbonate Transport - CO$_2$ Removal vs. Applied Current**

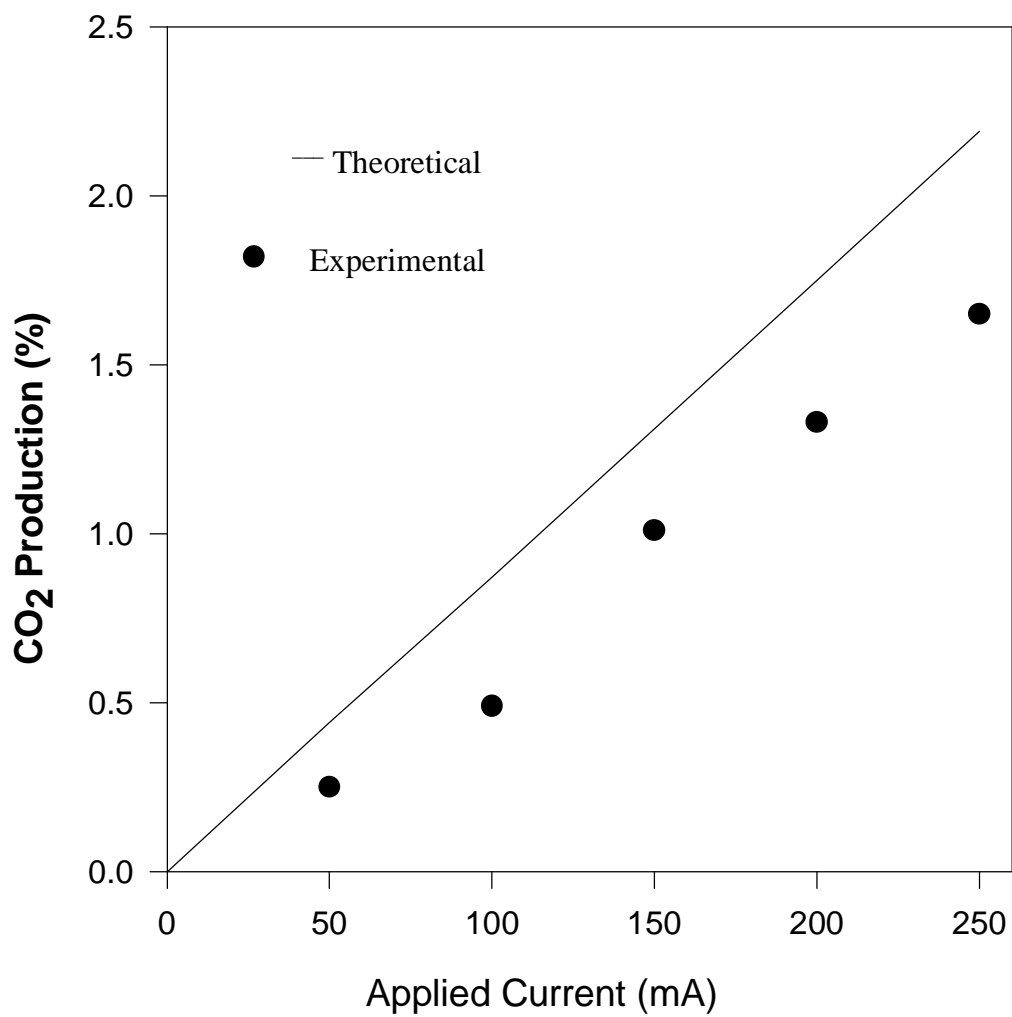# CO$_2$ Production vs. Applied Current



**Figure 15. Run #43. Carbonate Transport - CO$_2$ Production vs. Applied Current**
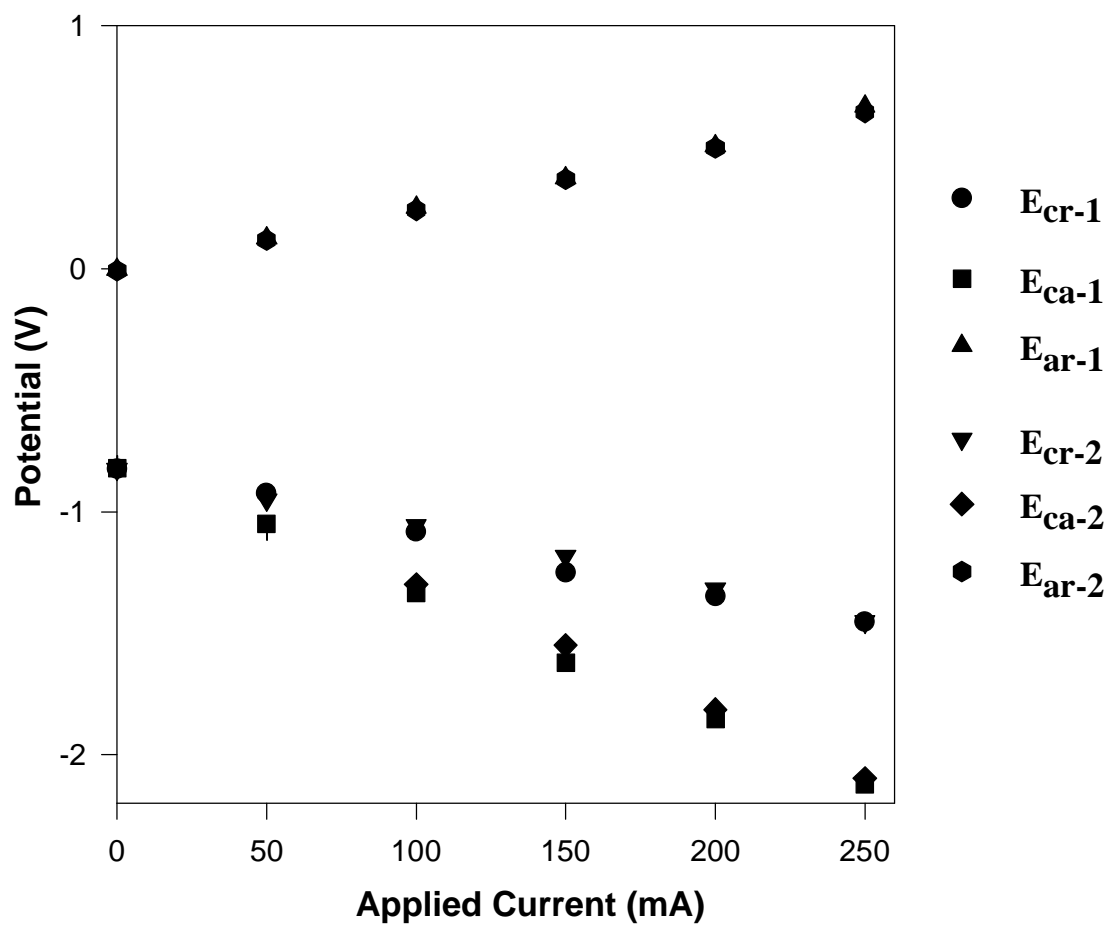
# Cell Potentials vs. Applied Current



**Figure 16. Run #43. Carbonate transport - Cell potential vs. Applied Current**

this is the first attempt at a full-cell run employing the $LiCoO_2$ electrode. This success at carbonate transport prompted attempts at $H_2S$ removal.

Removal of $H_2S$ from Sour Coal Gas

$H_2S$ removal was achieved utilizing the $LiCoO_2$ cathode at two different flow rates (135 cc/min and 320 cc/min) with a inlet $H_2S$ concentration of approximately 2500 ppm and at a temperature of 620 °C. At the cathode flow rate of 135 cc/min, the process gases equilibrated to: 4.48 % $CO_2$, 4.58 % CO, 8.09 % $H_2O$, 21.5 % $H_2$, 2717 ppm $H_2S$, 33 ppm COS, and balance $N_2$. Gas phase limiting current density was estimated at 32.2 mA/cm$^2$, while the membrane limiting current density was estimated at 126.4 mA/cm$^2$. The resulting molten electrolyte equilibrium was 88.3 % $M_2CO_3$ and 11.7 % $M_2S$.

Cathode flow was increased to 320 cc/min while maintaining the $H_2S$ inlet level around 2500 ppm. Process gases equilibrated to estimated values of: 3.71 % $CO_2$, 2.78 % CO, 8.13 % $H_2O$, 15.87 % $H_2$, 2375 ppm $H_2S$, 25 ppm COS, and balance $N_2$. Limiting current densities in the gas phase and membrane were 28.1 mA/cm$^2$ and 132.3 mA/cm$^2$, respectively. Molten salt equilibrium was estimated at 87.8 % $M_2CO_3$ and 12.2 % $M_2S$.

A current step was applied in both cases to determine the outlet $H_2S$ levels, % $H_2S$ removal, current efficiency, and the overpotential profile versus the applied current. Experiments were run twice at both flow rates to test for reproducibility. Figures 17-20 demonstrate these relationships, respectively. Figure 17 shows that $H_2S$ outlet concentrations drop with increasing applied current, as expected. This translates into increasing $H_2S$ removal with increasing applied current, as shown in Figure 18. Current efficiencies drop, however, with increasing applied current, as shown in Figure 19. These values would hopefully be improved upon cathode
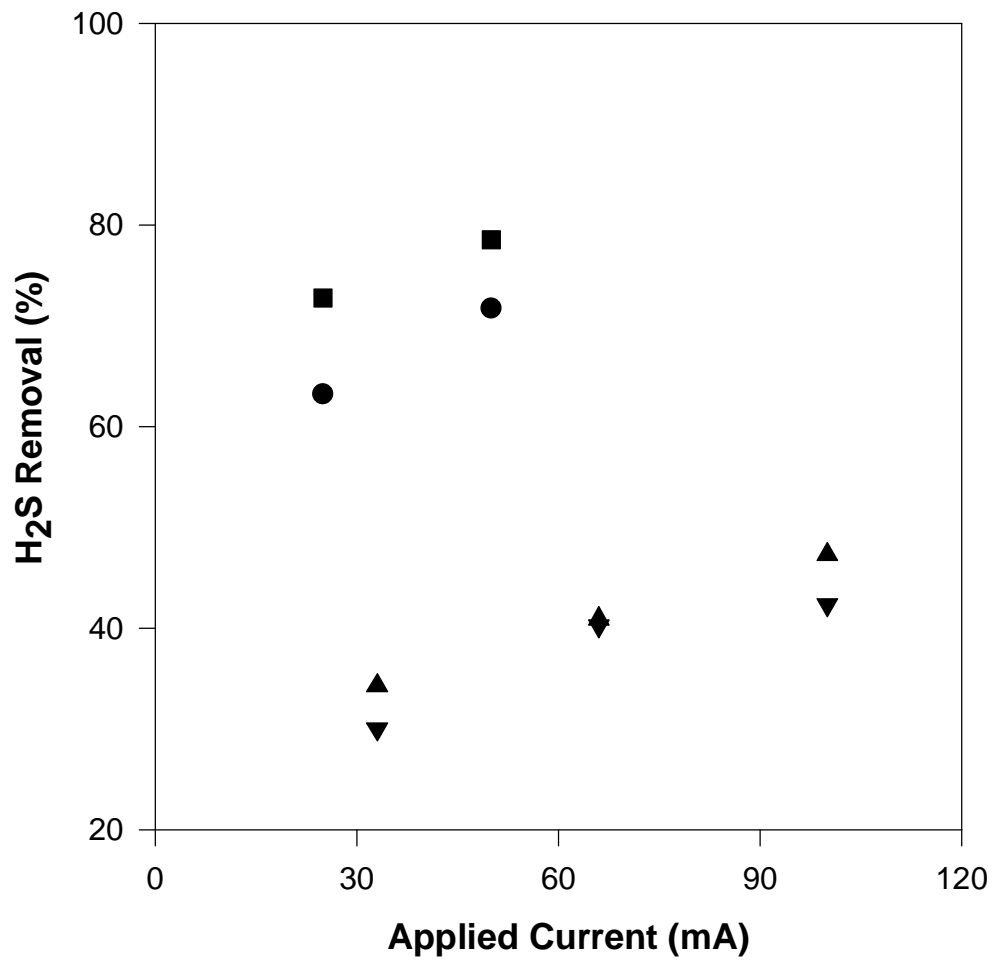
# H₂S outlet vs. Applied Current
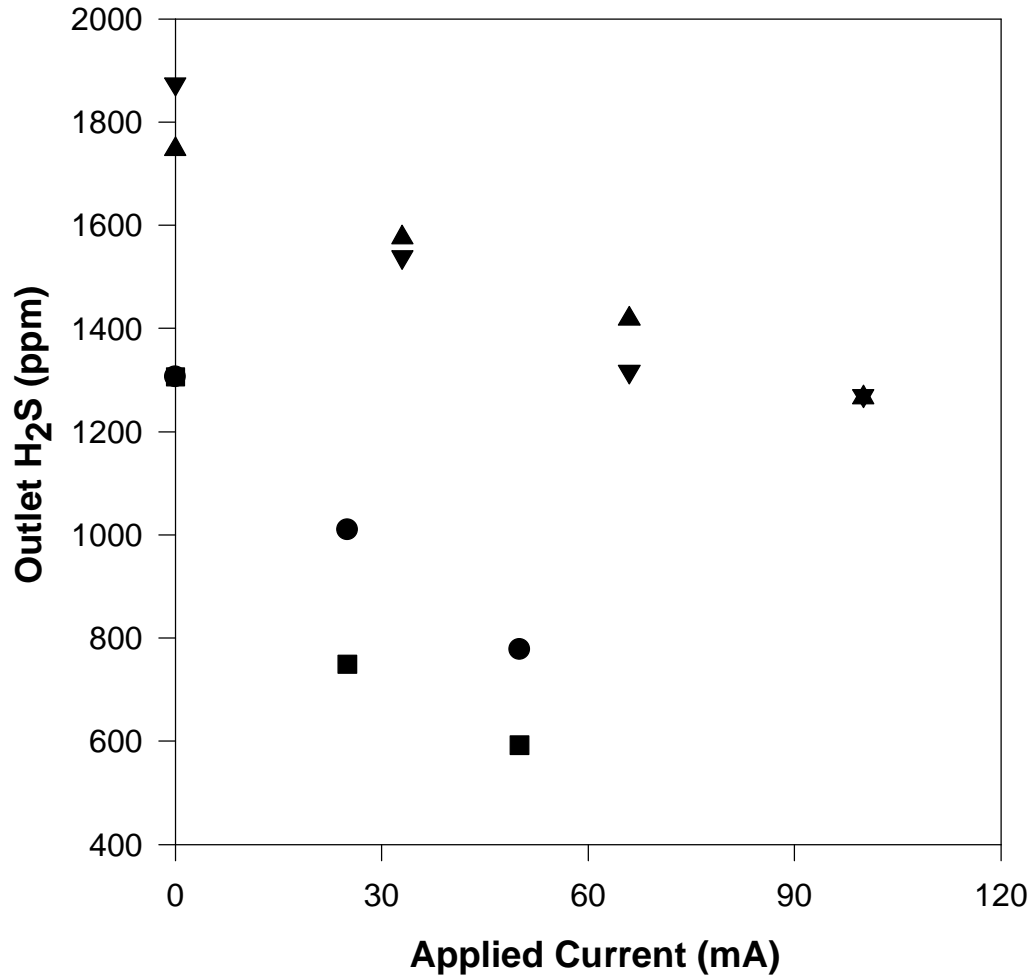


**Figure 17. Run #43. H₂S Outlet Concentration vs. Applied Current**

## H$_2$S Removal vs. Applied Current



- ●   **135 cc/min,2750 ppm H$_2$S inlet; trial 1**
- ■   **135 cc/min,2750 ppm H$_2$S inlet; trial 2**
- ▲   **320 cc/min,2300 ppm H$_2$S inlet; trial 1**
- ▼   **320 cc/min,2300 ppm H$_2$S inlet; trial 2**

**Figure 18.  Run #43.  H$_2$S Removal vs. Applied Current**
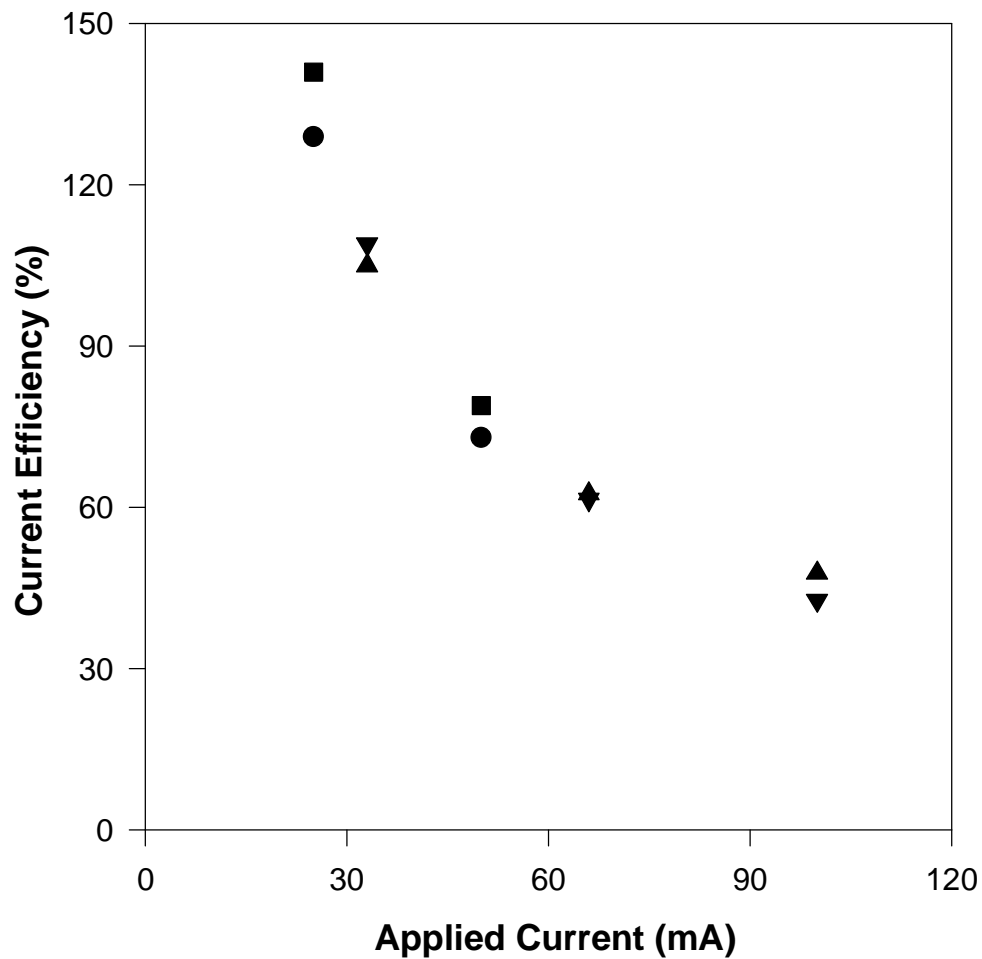
# Current Efficiency vs. Applied Current



Legend:
- ● 135 cc/min, 2750 ppm $H_2S$ inlet; trial 1
- ■ 135 cc/min, 2750 ppm $H_2S$ inlet; trial 2
- ▲ 320 cc/min, 2300 ppm $H_2S$ inlet; trial 1
- ▼ 320 cc/min, 2300 ppm $H_2S$ inlet; trial 2

**Figure 19.  Run #43.  Current efficiency vs. Applied Current**

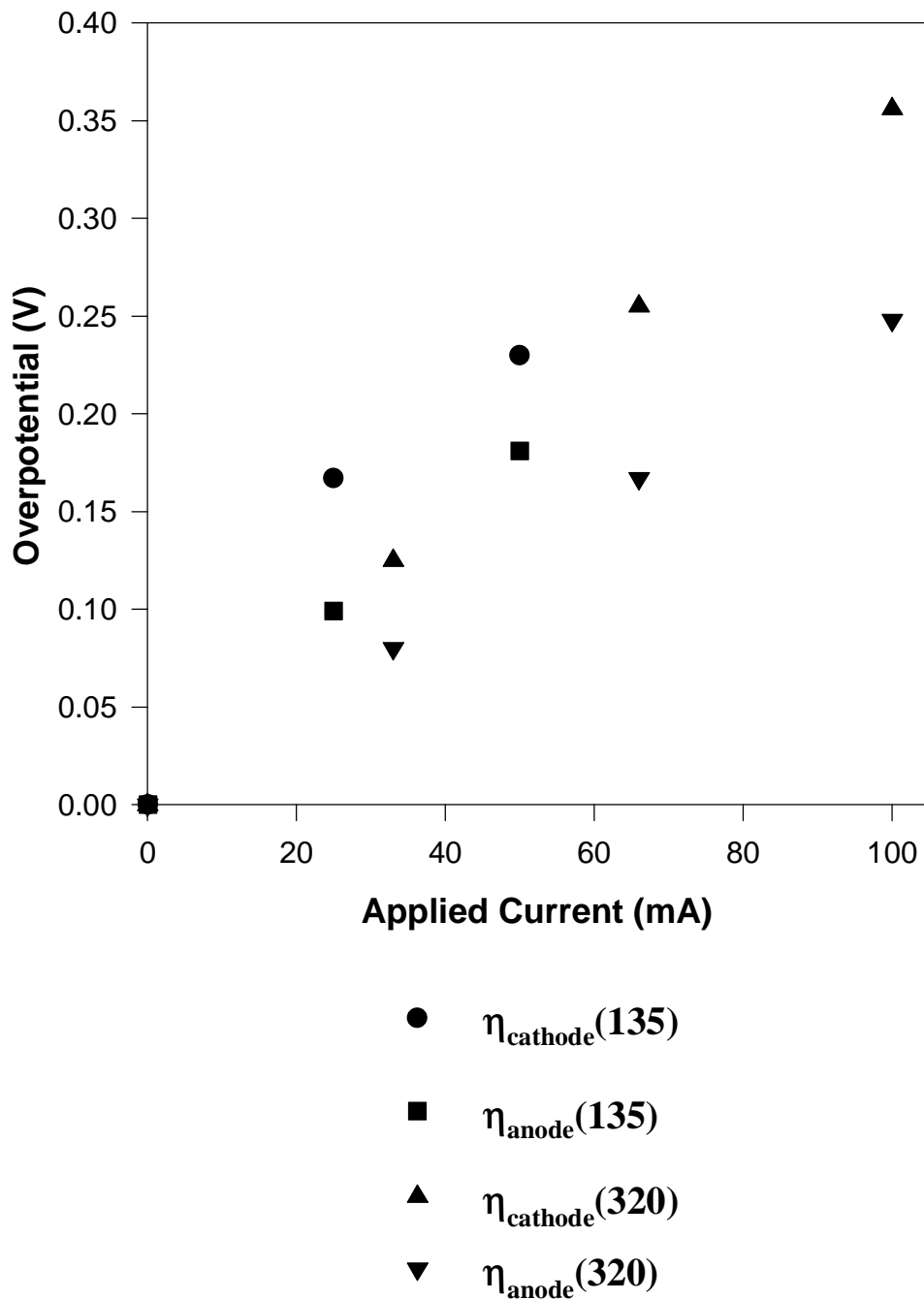# Electrode overpotential vs. Applied Current



Figure 20.  Run #43.  Electrode Overpotential vs. Applied Current

optimization, which entails fabricating an electrode with a pore distribution that favors wetting rather than flooding of the pores. Figure 20 illustrates that electrode overpotentials are within reasonable bounds, especially since these values have not been compensated for internal resistance, which ranged from 4 to 4.3 ohms. Better contact between the current collector and the electrodes should lower these overpotentials even further.

These results are very forward-looking considering that this was the first attempt with a $LiCoO_2$ electrode. The ability to run at 620 °C is a tremendous advantage over the nickel cathode, where temperatures are limited to 580 °C. As equation **(7)** illustrates, molten sulfide is formed with increasing temperature. Increased sulfide electrolyte concentrations enhance the removal of $H_2S$ because there is more sulfide available for oxidation. As previously stated, over 90 % $H_2S$ removal at >90 % current efficiencies has been achieved with a nickel cathode at 580 °C[15]. However, the ultimate goal of the removal cell is operation at 650 °C. Our first cell fun with an unoptimized $LiCoO_2$ cathode achieved successful $H_2S$ removal at 620 °C. Thus, cathode optimization should allow us to improve upon these results and increase the operating temperature to 650 °C.

Optimization of the cathode should improve upon these results tremendously. Before the full cell run, the pore-size distribution of the cathode was not known. Pores on the order of 5 microns are desired for electrode wetting. Smaller pores will flood and thus limit the sites available for $H_2S$ reduction. This may have been one reason for decreasing current efficiency at higher applied currents. Also, electrolyte mismanagement is somewhat to blame for pore

flooding. Post-mortem analysis revealed that the cathode flow chamber was flooded with $K_2SO_4$, as has happened in past experiments due to excess electrolyte addition.

X-ray diffraction of the cathode after the cell run is shown in Figure 21. The figure indicates that $LiCoO_2$ is present in the cathode cell run. In fact, this analysis contradicts the aforementioned earlier $LiCoO_2$ powder/$H_2S$ gas flow study. A possible explanation for this is the carbonate environment which may help stabilize $LiCoO_2$ in the presence of $H_2S$. More studies will be performed to determine the interactions of this environment. Additionally, the post full cell run cathode existed as one piece. It did not disintegrate as is common for the nickel cathode after full cell runs. This is a positive result which indicates that the cathode remained in the solid state throughout the duration of the experiment.

Figure 21. X-Ray Diffraction of $LiCoO_2$ Cathode after Run #43
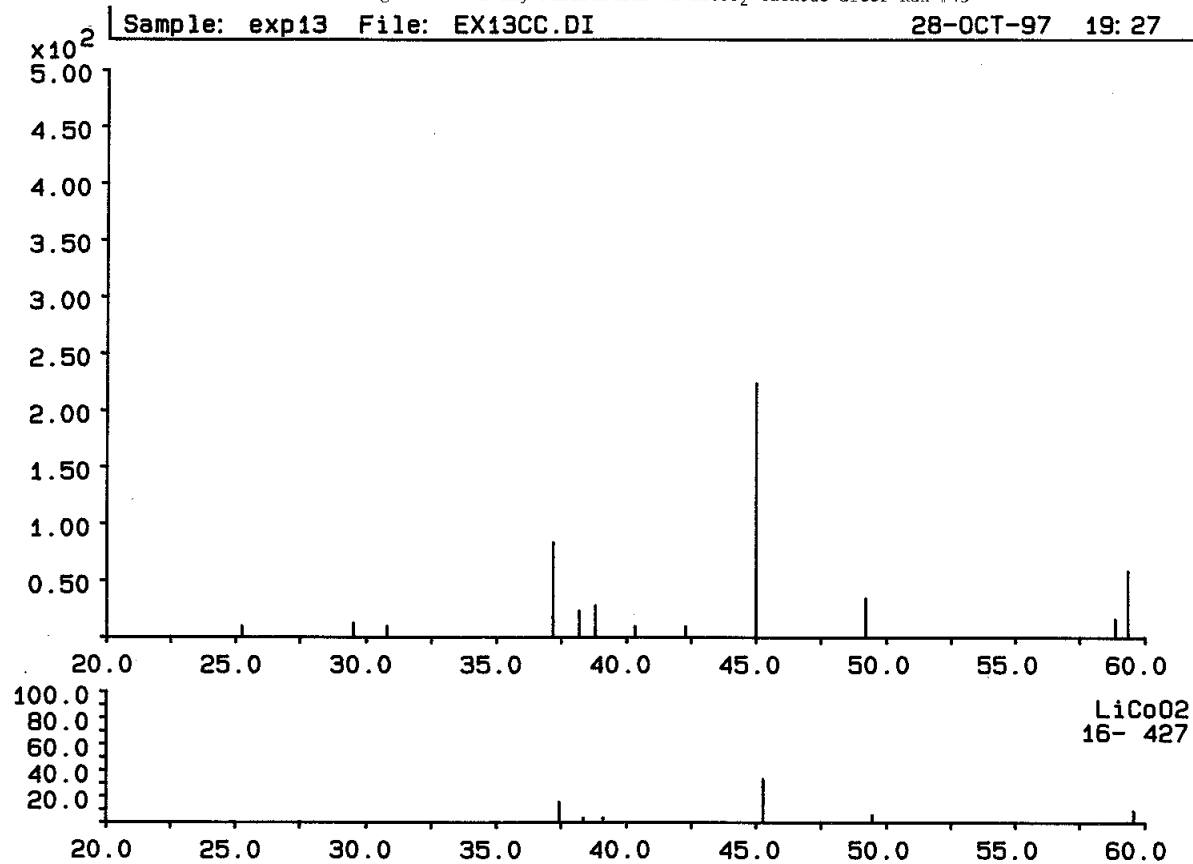
## Conclusion

This quarter's research focused on two areas - stainless steel aluminum passivation and an alternate cathode to replace Ni, $LiCoO_2$. Stainless steel cell housings coated with aluminum demonstrated capability at both carbonate transport and $H_2S$ removal. These are the best results achieved to date utilizing passivated stainless steel cell housings with a sour gas. The passivation layer provides a nonconductive layer on top of the stainless steel housings which eliminate parasitic reactions. Low current efficiencies are probably due to electrolyte mismanagement rather than parasitic reactions at any exposed stainless steel surface.

$LiCoO_2$ was determined to be a successful alternative to the Ni cathode. Stoichiometric carbonate transport was achieved with electrodes fabricated from this material. In addition, $H_2S$ removal was demonstrated at a temperature of 620 °C. Moreover, post-mortem X-ray diffraction patterns of this cathode showed that it was resistant to the strong sulfurizing environment . This was the first attempt utilizing $LiCoO_2$ as the cathode. While $H_2S$ removal and current efficiencies weren't as successful as for nickel cathodes at 580 °C, $LiCoO_2$ is preferred over nickel because it can be operated at 650 °C. It is anticipated that $LiCoO_2$ cathode optimization will improve upon these encouraging results.

## Projected Work

This quarter, full cell runs with aluminum passivated stainless steel cell housings will be continued, with strong emphasis on managing the amount of additional electrolyte. The effect of $Al_2O_3$ aerosol applied on the aluminum covered cell housings will also be studied. In addition, cell housings which are plasma coated with $Al_2O_3$ rather than aluminum will be ordered from

Plasma Coatings, Inc. It is anticipated that these nonconductive coatings will eliminate any possibility of carbonate oxidation at any exposed stainless steel surface.

Research into $LiCoO_2$ as a possible cathode material will also be continued. This quarter, the effect of the carbonate environment combined with the presence of $H_2S$ will be studied in $LiCoO_2$ powder test as well as full cell runs. Electrode fabrication will also be optimized for sintering conditions and pore size distribution. Various factors will need to be optimized, including: initial amount of poreformer, initial particle size, dry pressing techniques, and sintering times and temperatures, among others. SEM and mercury porosimetry should provide insight to the optimization process. Fabricated $LiCoO_2$ electrodes will be utilized in full cell removal experiments at 650 °C.

## References

1. U.S. Dept of Energy, DOE/METC 87/0255, DE87006493, Oct., 1987.

2. Skerret, P.J., "Fuel Cell Update", *Popular Science*, 89-91, 120-1, June, 1993.

3. Lim, H.S. and Winnick, J., *J. Electrochem. Soc.*, **131, 562-8** (1984).

4. Alexander, S., and Winnick, J., *1990 AIChE Annual Meeting*, Chicago, IL., 1990.

5. Alexander, S., and Winnick, J., *Sep'n Sci. and Tech.*, **25**, 2057-72 (1990).

6. Weaver, D., and Winnick, J., *J. Electrochem. Soc.*, **134**, 2451-58 (1987).

7. Weaver, D., and Winnick, J., *J. Electrochem. Soc.*, **138**, 1626-37 (1991).

8. Banks, E., and Winnick, J., *J. Appl. Electrochem.*, **16**, 583-90 (1986).

9. White, K.A., and Winnick, J., *Electrochim. Acta*, **30**, 511-516 (1985).

10.  EPRIEM-1333, *Assessment of Sulfur Removal Processes for Advanced Fuel Cell Systems, Final Report,* C.F. Braun and Co., Alhambra, CA, Jan., 1980.

11.  Vidt, E.J., DOE/METC DE-AC-21-81MC16220, DE82013942, Westinghouse, Dec., 1981.

12.  Focht, G.D. et. al., DOE/MC/121166-2163, DE86016041, July, 1986.

13.  Lyke, S.E., DOE/MC/19077-1803, DE8500961, Battelle Pacific Northwestern Laboratories, Jan. 1985.

14.  Alexander, S., Ph.D. Thesis, Georgia Institute of Technology, 1993.

15.  Winnick, J., DOE Quarterly Report - Contract #DE-FG22-94-PC94207, April, 1996.

16.  Giorgi, L., Carewska, M., Patriarca, M., Scaccia, S., Simonetti, E., and Di Bartolomeo, A., *Journal of Power Sources*, **49**, 227-43 (1994).

17.  Tennakoon, T.M., Lindbergh, G., and Bergman, B., *J. Electrochem. Soc.*, **144**, 2296-2301 (1997).

18.  Lagergren, C., Lundblad, A., and Bergman, B., *J. Electrochem. Soc.*,**141**, 2959-66(1994).